

REVIEW

Crystalline porous materials for catalytic conversion of lignin-related substances

Qing Huang^{1,2} | Pengfei Wu³ | Xiu-Fen Li² | Yi-Rong Wang² | Dan Tian¹ | Ya-Qian Lan² ¹College of Materials Science and Engineering, Nanjing Forestry University, Nanjing, Jiangsu, P. R. China²School of Chemistry, South China Normal University, Guangzhou, P. R. China³Co-Innovation Center for Sustainable Forestry in Southern China, Nanjing Forestry University, Nanjing, Jiangsu, P. R. China

Correspondence

Dan Tian, College of Materials Science and Engineering, Nanjing Forestry University, Nanjing 210037, Jiangsu, P. R. China.
Email: tiandan@njfu.edu.cnYa-Qian Lan, School of Chemistry, South China Normal University, Guangzhou 510006, P. R. China.
Email: yqlan@m.scnu.edu.cn

Funding information

National Natural Science Foundation of China, Grant/Award Numbers: 22101089, 22225109, 22175094, 21871141, 21871142, 22071109, 92061101; Guangdong Basic and Applied Basic Research Foundation, Grant/Award Number: 2020A1515110836; Open Fund of Energy and Materials Chemistry Joint Laboratory of SCNU and TINCI, Grant/Award Number: SCNU-TINCI-202204

Abstract

The conversion of the biomass into eco-friendly fuels and chemicals has been extensively recognized as the essential pathway to achieve the sustainable economy and carbon neutral society. Lignin, as a kind of promising biomass energy, has been certified to produce the high-valued chemicals and fuels. Numerous efforts have been made to develop various catalysts for lignin catalytic conversion. Both metal-organic frameworks (MOFs) and covalent organic frameworks (COFs) belong to very important heterogeneous porous catalysts due to their regular porous structures, high specific surface area, and precisely tailored diversities. In the review, the first part focused on the catalytic conversion of lignin, lignin model compounds, and lignin derivatives using the pristine MOFs, functional MOF composites, and MOF-derived materials. The second part summarized the catalytic conversion of lignin model compounds using pristine COFs and functional COF composites. The review here mainly concentrated on the design of the materials, screening of catalytic conditions, and explorations of the corresponded mechanisms. Specifically, (1) we summarized the MOF- and COF-based materials for the effects on the catalytic transformation of lignin-related substances; (2) we emphasized the catalytic mechanism of C–C and C–O bonds cleavage together with the structure–activity relationships; (3) we in-depth realized the relationship between the chemical/electronic/structural properties of the MOF- and COF-based catalysts and their catalytic performance for lignin-related substances. Finally, the challenges and future perspectives were also discussed on the catalytic conversion of lignin-related substances by MOF- and COF-based catalysts.

KEYWORDS

catalytic conversion, covalent organic frameworks, lignin, lignin derivatives, lignin model compounds, metal-organic frameworks

1 | INTRODUCTION

As the crisis of diminishing fossil fuels and deteriorating environmental pollutions, many tremendous efforts have been implemented to design novel routes for producing value-added chemicals and liquid fuels, especially depolymerizing biomass raw materials into the energy products directly.^[1–10] The lignin, as a kind of great candidate for green and sustainable chemicals and liquid fuels, was an amorphous polymer consisting of phenylpropane units connected through carbon–carbon and ether bonds.^[11–14] Lignin recently has been considered as the second-largest biomass

resources preceded after cellulose in the plant kingdom, accounting for 15%–25% of the total lignocellulosic. However, recently it is treated as waste or simply combusted, and has not been adequately utilized.^[15–17] In most plants, guaiacyl (G), syringyl (S), and p-hydroxyphenyl (H) are common phenylpropane units constructing lignin. The decomposition of lignin macromolecules into monomer components provides opportunities for the production of high-value aromatic products. However, the highly active depolymerization of lignin with complex structural characteristics into valuable compounds has become a recognized challenge.^[2,18] One of the obstacles hindering the efficient depolymerization of lignin might be the compact structural integrity. Despite that C–O–C and C–C bonds initiated the linkage of

Qing Huang and Pengfei Wu contributed equally to this study.

This is an open access article under the terms of the [Creative Commons Attribution](https://creativecommons.org/licenses/by/4.0/) License, which permits use, distribution and reproduction in any medium, provided the original work is properly cited.

© 2024 The Authors. *Aggregate* published by SCUT, AIEI, and John Wiley & Sons Australia, Ltd.

phenylpropane units, the strong electronic densities of these units were also benefit for the compact integrity and stability of the macromolecules.^[19–21] On the urgent demand for the substitute sustainable energy and fine chemicals, the lignin degradation has drawn extensively attentions for obtaining the highly valued fuels or small molecules.^[2,22] A common method for the lignin degradation is breaking the C–O bonds in β -O-4 ethers, taking $\sim 50\%$ of the structures. The two-stage procedures generally selectively oxidate the benzyl β -O-4 alcohol to benzyl β -O-4 ketone, and subsequently reduced by cleaving the C–O bonds, finally resulting in the formation of high-valued energy products. The use of catalysts will significantly improve the efficiency of the lignin conversion process. Recyclable heterogeneous catalysts are widely applied in hydrogenolysis and hydrodeoxygenation (HDO) reactions of lignin due to their tunable chemical/physical properties.^[23] The main heterogeneous catalysts used for lignin-related substances are noble metals (Pd, Ru, Rh, etc.), transition metals (Ni, Co, W, Mo, etc.), metal oxides (MoO_x , ReO_x , etc.), and crystalline porous materials (metal-organic frameworks [MOFs], covalent organic frameworks [COFs], etc.).

MOFs skillfully combined the organic ligands and metal nodes via coordination bonds, forming the porous network structures. The high specific surface area and tunable structure–functionality enabled MOFs with widely applications in various fields, such as adsorption, separation, catalysis, pharmaceuticals, etc.^[24–30] In particular, the metal nodes and organic ligands in MOFs can provide a wealth of active sites and functional properties for acting as the heterogeneous catalysts, catalyst carriers, and even precursors with excellent catalytic properties.^[10,31–33] In contrast to other heterogeneous catalysts, the tunable porosity and high specific surface area can facilitate the diffusion of biomass molecules to access the active sites, especially tunable pore size and pore environment allow the MOFs to improve the selectivity of target products. Multiple functional sites (different functional molecules, metal sites, and metal clusters) can be integrated into a single MOF to enhance catalytic activity, thereby successfully preparing them as the multifunctional catalytic materials. Without changing their frameworks, the catalytic activity of MOFs could be modulated by adjusting the electronic structure, which also could be modified through metal ion doping or functionalization of organic ligands. On this condition, the controllable characters of MOFs could be easily synthesized into a variety of nanostructures, such as 1D nanorods, 2D ultrathin nanosheets, nanoflowers, etc. Furthermore, the MOFs could be a basis for preparing other functional materials in/on their pores/surfaces. As these reasons, a large number of MOF-based catalysts were developed and the related studies have always been at the forefront of research in the field of biomass conversion in the recent few years, including some progresses in the fields of lignin, its model compounds, and derivatives.^[7,34–37]

COFs are a class of crystalline porous materials, being capable of integrating organic units into highly sequenced materials through dynamic covalent chemistry.^[38,39] COFs generally contain the low density and high chemical and thermal stability. Similar to MOFs, the structures, pore sizes, shapes, and functions of COFs could be also modulated through pre-designed functional monomers with appropriate rigidity and directionality. Meanwhile, the condensation of these monomers usually requires a certain degree of

reversibility to obtain highly ordered structures. Those bonds with a certain degree of activity generally produce a crystalline structure with permanent porosity. Applying the knowledge of topological maps and different covalent polycondensation, reactions can design and construct the aimed COFs with specific physicochemical characteristics, including the shapes, interfaces, pore sizes, shapes, and environments.^[40–42] The covalent bonds in COFs can be classified as hydrazine and azine-,^[43–53] imine-,^[54–73] amide-,^[58,74,75] C(sp³)-N-,^[76–80] boroxine- and boron ester-,^[81–89] cyanovinylene-,^[90] and olefin-linked COFs.^[91–99] According to the dimensional array of the frameworks, COFs can be categorized as 2D or 3D materials.^[40,41] In contrast to other polymers and porous materials, the polygonal skeleton is the main characteristic of COFs, providing great opportunities for the design and development of a new class of functional porous materials. In recent years, COFs have also attracted extensive attention in the academic field according to their excellent thermal and chemical stability, adjustable pore structure, easy surface modification, structural versatility, flexible/tunable chemical monomer combination, etc.^[40,42,100–105] The wide applications of COFs make the materials promising candidates in the gas storage and separation, heterogeneous catalysis, drug delivery, proton conduction, Li-ion battery, energy storage, conversion, etc. These structural and functional properties are similar to MOFs.^[106–110] Meanwhile, COFs with the strong covalent bonds exhibited higher stability under acidic and alkaline conditions, increasing the potential in heterogeneous catalysis.

MOFs and COFs, as the typical crystalline porous materials, are of great interest in the catalytic conversions of lignin-related substances due to their high porosity, large specific surface area, and tunable structure–function. In general, high specific surface area and porosity facilitate the adsorption and diffusion of lignin-related substrates while providing more accessible active sites. The tunable structure means that the designable possibility of functionally oriented synthesis promotes the activation of functional groups around the C–O and C–C bonds in lignin-related substrates, thereby being benefit for further cleavage of the C–O and C–C bonds, and finally improving the catalytic activity and selectivity. Metal sites and organic linkers can provide abundant active sites and functional properties to facilitate the catalytic conversion of lignin-related substrates by MOFs and COFs. Furthermore, the inherent porous framework structures and tunable assembly environments allow them as excellent carriers to compound with other materials, and fully utilize the functional synergies and enhance the lignin-catalyzed efficiency. In addition, they can be used as excellent precursors to prepare functional materials with different shapes, sizes, and defects derived from the original inorganic and organic components, which are expected to improve the performance of lignin catalytic conversion.

The study reviewed the catalytic conversion of lignin-related substances by MOF- and COF-based materials, including pristine MOFs and COFs, functionalized MOF and COF composites, MOF-derived materials (Figure 1). Although several reviews summarized the MOF materials for the catalytic conversion of biomass, it still lack a comprehensive and systematic summary focused on the conversion of lignin-related substances by MOF-based materials. At

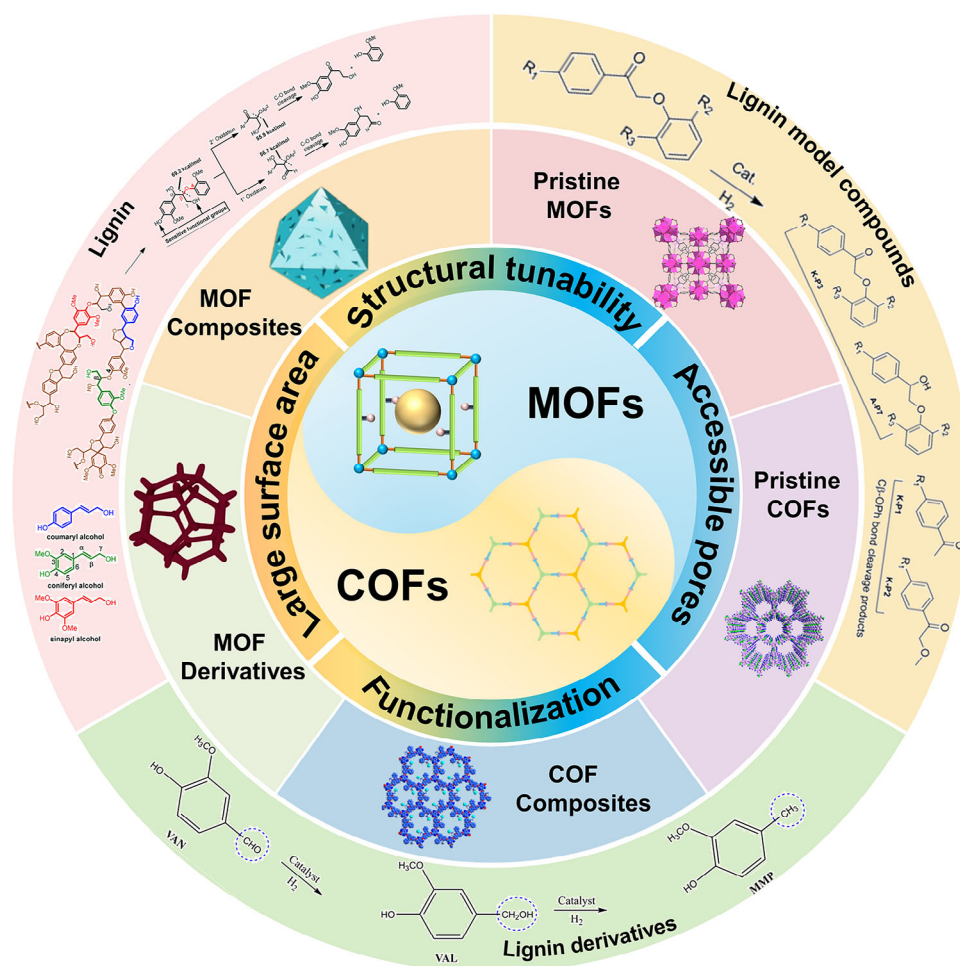


FIGURE 1 Schematic illustration of crystalline porous materials for catalytic conversion of lignin-related substances.

present, the catalytic conversion of lignin-related substances by COF-based materials is still in its infancy stage, even no related review reports their conversion. Therefore, an overview is urgently needed to discuss the research progress of lignin-related substances by MOF- and COF-based materials, according to the complexity of the catalytic system, ranging from pristine MOFs and COFs to their functionalized composites and derived materials. In this review, we first focused on the catalytic conversion of pristine MOFs, functionalized MOF composites, and MOF-derived materials for lignin, lignin model compounds, and lignin derivatives. Then, the applications of pristine and functionalized COFs on catalytic conversion of those lignin-related substances were also summarized and discussed. Meanwhile, a comprehensive summary was made from the aspects of material design, screening of catalytic reaction conditions, catalytic performance, and catalytic mechanism.

2 | CONVERSION OF LIGNIN, ITS MODEL COMPOUNDS, AND DERIVATIVES BY MOF-BASED MATERIALS

Owing to the porous nature, structural and functional tunability of MOF-based materials, they become the superior candidates applied in the catalytic conversion of lignin-related substances. These candidates could be categorized as the following three types: the pristine MOFs, MOF com-

posites, and MOF-derived materials. As illustrated in the timeline, Figure 2 exhibits a series of recent progress that have been made in the catalytic conversion of lignin, its model compounds, and derivatives by MOF-based materials. Early work gradually utilized the confinement effect of MOFs to load metal nanoparticles (NPs) for hydrogenation of lignin-related substances. In 2015, Xu and coworkers successfully prepared Pd@MIL-101 for the first time by immobilizing ultrafine Pd NPs in MOF pores as a high active and durable catalyst for vanillin (VN) HDO.^[111] Such high catalytic performance could be attributed to the nano-confinement effect and the strong interaction between Pd NPs with reactants. Also in 2015, a multiphase tandem catalyst [Pd/SO₃H-MIL-101(Cr)] was prepared for product upgrading in the HDO reaction of lignin-derived VN.^[37] This excellent efficiency mainly owed to both the uniform dispersion of Pd NPs and the induced activation of reactants by sulfonic acid groups. In addition to precious metals, MOFs loaded with non-precious metals could also achieve catalytic conversion of lignin-related substances, such as Ni and Ti. Allendorf and coworkers found that MOF-based materials also displayed activity for the catalytic hydrogenolysis of C–O bonds in lignin-related substances. Mg-IRMOF-74(I) and Mg-IRMOF-74(II) selectively catalyzed the cleavage of β-O-4-containing α-O-4 and 4-O-5 bonds of phenyl ethers to generate the corresponding hydrocarbons and phenolic products.^[112] Afterwards, Cai and coworkers achieved highly active catalysis of self-hydrogen transfer hydrogenolysis of

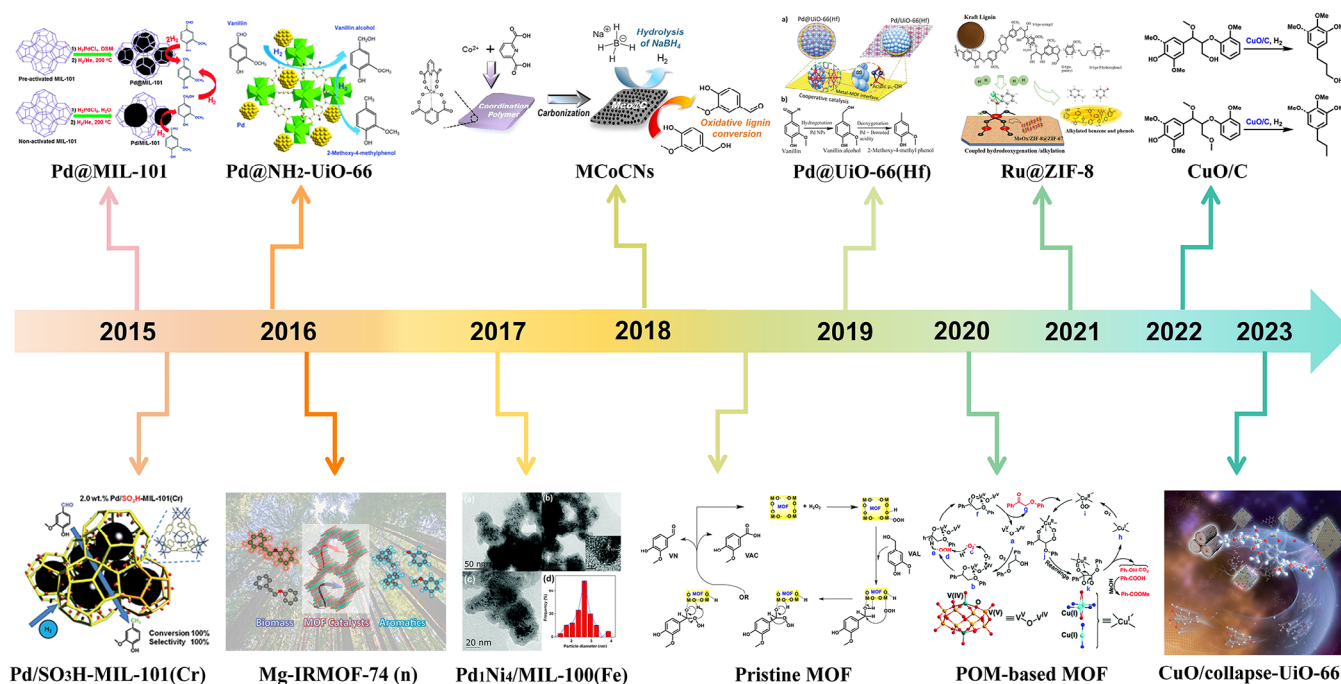


FIGURE 2 Evolution timeline of metal-organic framework (MOF)-based materials in catalytic conversion of lignin-related substances. (2015): Pd@MIL-101 for hydrodeoxygenation (HDO) of vanillin (VN). Reproduced with permission: Copyright 2015, Royal Society of Chemistry.^[111] (2015): Pd/SO₃H-MIL-101(Cr) for HDO of VN. Reproduced with permission: Copyright 2015, Royal Society of Chemistry.^[37] (2016): Pd@NH₂-UiO-66 for HDO of VN. Reproduced with permission: Copyright 2016, Royal Society of Chemistry.^[35] (2016): Mg-IRMOF-74 (n) for cleavage of phenyl ethers containing β -O-4, α -O-4, and 4-O-5 linkages. Reproduced with permission: Copyright 2016, American Chemical Society.^[112] (2017): Pd₁Ni₄/MIL-100(Fe) for the intramolecular hydrogen transfer C–O cleavage of lignin model compounds. Reproduced with permission: Copyright 2017, Royal Society of Chemistry.^[113] (2018): MCoCNs for oxidative conversion of vanillyl alcohol (VAL). Reproduced with permission: Copyright 2018, Elsevier.^[119] (2018): pristine MOF for oxidation of VAL. Reproduced with permission: Copyright 2018, Springer Nature.^[117] (2019): Pd@UiO-66(Hf) core–shell for VN HDO reaction. Reproduced with permission: Copyright 2019, Royal Society of Chemistry.^[114] (2020): polyoxometalate (POM)-based MOF for catalytic conversion of β -O-4 lignin model compounds. Reproduced with permission: Copyright 2020, Royal Society of Chemistry.^[118] (2021): Ru@ZIF-8 for selective hydrogenolysis of C–O bonds in lignin model compounds. Reproduced with permission: Copyright 2021, Royal Society of Chemistry.^[115] (2022): MOF-derived CuO/C catalyst for hydrogenolysis of lignin into monomeric phenols. Reproduced with permission: Copyright 2022, Royal Society of Chemistry.^[121] (2023): CuO/collapse-UiO-66 for catalytic deconstruction of lignin into phenolic monomers. Copyright 2023, American Chemical Society.^[120]

lignin model compounds and organosolv lignin using Pd–Ni bimetallic NP-loaded MIL-100(Fe) catalysts. The selective cleavage of β -O-4 bonds in lignin was achieved without additional hydrogen donors by utilizing the C α H–OH group in lignin as a hydrogen source.^[113] A series of similar work followed using MOFs as framework carriers loaded with metal NPs or other materials for the catalytic transformation of lignin-related substances explored the synergistic effects and catalytic mechanisms.^[35,114–116] In 2018, the pristine MOF materials, such as MIL-101(Cr), MIL-101(Fe), UiO-66, HKUST-1, and MOF-801, and other crystalline materials began to be applied in catalyzing vanillyl alcohol (VAL) to VN and vanillic acid (VAC), which also systematically investigated the effects of time, catalyst type, metal fraction, oxidant content, and pH value on the catalytic reactions.^[117] Successively, Liu et al. catalyzed the cleavage of β -O-4 and C–C bonds of lignin model compounds by the pristine polyoxometalate (POM)-based MOF, and investigated the function of the mixed-valent V^V–O–V^{IV} and Cu(I) active sites.^[118] In 2018, Lin and coworkers started to synthesis the carbonized materials by utilizing MOF as precursors for the catalytic transformation of lignin-related substances. The carbonized cobalt/carbon nanomaterials (MCoCNs) oxidized the VAL to VN with a selectivity of more than 99%.^[119] In 2023, CuO/c-collapse-UiO-66 catalysts was developed for the reductive hydrogenolysis of poplar lignin with the monophenol yields up to 42.8 wt%. The C–O bond cleavage process was

facilitated via the synergistic effect of the acid/base sites of the catalyst.^[120] During this period, many efforts were also invested in the preparation of different metal-doped C and N nanomaterials by using MOFs as precursors for the catalytic conversion of lignin-related substances,^[121–123] and further explored the catalytic activities and synergistic effects of different inorganic and organic components. The corresponded results supply new opportunities for the development of MOF-based catalysts with high performance.

2.1 | Conversion of lignin, its model compounds, and derivatives by pristine MOFs

Lignin with a complex structure is a kind of natural macromolecules, and difficult to be degraded. The pristine MOFs showed certain catalytic activity in the field of catalytic conversion of lignin-related substances. Although the pristine MOFs are hard for the conversion of natural lignin, they exhibited high activity and selectivity in the catalytic conversion of some lignin model compounds due to their high specific surface area, controllable pores, and functional characteristics. More importantly, the use of pristine MOFs for the catalytic transformation of lignin model compounds will help to investigate their catalytic mechanisms (including cleavage of C–O and C–C bonds) at the molecular level due to their well-defined molecular structures. In recent years, pristine

MOFs have gradually begun to be developed and utilized for the catalytic studies of lignin model compounds and lignin derivatives.

VAL originates from the second-largest biomass materials, containing the benzene rings, methoxy groups, phenolic hydroxyl groups, and alcoholic hydroxyl groups. It is also a representative β -O-4 lignin model compound that can be converted into many valuable products (such as VN, VAC, or guaiacol [GAL]).^[117] These products can be used in chemical pharmaceuticals, food additives, perfume preparations, and other fields. The conversion of VAL was widely documented by some common and typical MOFs. For example, Lin et al. successfully oxidized VAL to produce VN, VAC, and GAL by MIL-101(Cr), MIL-101(Fe), UiO-66, HKUST-1, and MOF-801 under the microwave catalytic oxidation.^[117] The work mainly discussed the oxidation reaction effects of VAL from the aspects of MOF type, hydrogen peroxide dosage, reaction temperature, solvent, and pH value. Interestingly, some MOFs with higher specific surface area did not show the corresponded conversion efficiency (e.g., MIL-101(Cr), MIL-101(Fe), and HKUST-1), while MOF-801 with moderate specific surface area exhibited the best conversion rates of VAL and maximum yield of VN and VAC in acetonitrile solvent. Furthermore, the various metal clusters even with same ligand could also result in various VN and VAC yields, including MIL-101(Cr), MIL-101(Fe), and UiO-66 catalysts. The solvent experiments indicated that the polarity of the solvent could also affect the interaction between the reactants and MOFs, which finally led to the production of different intermediates.^[124] The temperature experiments showed that higher temperature was not necessarily beneficial for the conversion of VAL, as more intense reactions might decompose VAL. The pH experiments meant that the alkaline environment seemed to be beneficial for the reaction process. The participation of hydrogen peroxide in the experiments indicated that higher hydrogen peroxide did not necessarily favor the conversion of VAL, but promoted the generation of VAC through the oxidation property.

The involvement of hydrogen peroxide indicated that the conversion mechanism of VAL by MOFs might be related to $\text{OH}\cdot$. The $\text{OH}\cdot$ first oxidized VAL to produce VN, and then converted into VAC or GAL.^[125] Among them, the catalytic mechanism of MIL-101(Cr) and HKUST-1 belonged to the model involving $\text{OH}\cdot$. In converting VAL to VN/VAC reaction, MOF-801 showed higher conversion efficiency than MIL-101, but MOF-801 did not exhibit a strong $\text{OH}\cdot$ signal. Meanwhile, UiO-66 did not show a strong $\text{OH}\cdot$ signal, but VAL could still be converted into VN/VAC using these two MOFs. This suggested that there might be other pathways for converting VAL in these two MOFs.^[126] It has been reported that metal oxides could react with hydrogen peroxide via non- $\text{OH}\cdot$ pathways to convert VAL to VN and VAC, as shown in Figure 3A.^[127] When MOFs reacted with hydrogen peroxide, the hydrogen peroxide might be dissociated to produce hydroperoxyl group and protic hydrogen, which could further interact with the metal-oxygen clusters of MOFs. Electron-rich hydroperoxyl group might react with the ortho-carbon and ortho-hydrogen of hydroxyl group to form activated oxygenic intermediates, and then reacted with alcohol to form water. At the same time, vanilloxy cation could release a proton, then reacted with the O of the hydroperoxyl group to produce the target VAC. However,

there might be another pathway in which the oxygen-enriched hydroperoxyl group reacted with the proton on the activated oxygenic intermediate, producing another compound (VN).

In view of the relatively low VAL conversion rate and VN product selectivity of the hydrogen peroxide system,^[127–129] other oxidants tried to achieve the efficient conversion of VAL to VN.^[130–132] Typically, 2,2,6,6-tetramethylpiperidine-1-oxyl (TEMPO) was used as an oxidizing agent to efficiently convert VAL into VN.^[117,125,133,134] Lin et al. introduced polyvinylpyrrolidone (PVP) as a capping agent not only changed the size of HKUST-1, but increased the hydrophilicity of the catalyst, improving more opportunities to contact VAL substrate molecules.^[134] In the case of TEMPO as the oxidizing agent, the yield efficiency of VAL to VN could reach 91% within 2 h, and the selectivity achieved as high as 100%. It is unrecyclable for TEMPO used in the traditional Cu/TEMPO catalytic systems.^[135] For easier recycling of the catalysts and oxidants, Lin et al. further designed a more advanced catalytic system by both using copper mesh as source to directly grow HKUST-1 (as catalysts) and utilizing the carbon cloth to graft TEMPO (TEMPO@CC) (as oxidants) (Figure 3B).^[132] Macroscopic mesh substrates allow reaction substrates to pass through more easily than ordinary substrates. Once the reaction substrate contacted the catalyst on the copper grid and TEMPO@CC simultaneously, a sandwich-like catalyst system (SCS) is formed. At 120°C, SCS could convert VAL to VN at 100% conversion rate and 100% VN selectivity in 1 h. Since the conversion of VAL to VN was a thermochemical reaction, the heating process was critical. The authors further investigated the effects of conventional oven heating (COH) and microwave irradiation (MWI) heating methods on the catalytic reaction (Figure 3C). There was almost no VAL conversion when the HKUST-1 mesh was present alone under both methods. TEMPO@CC exhibited low conversion rate under both methods. When TEMPO@CC and HKUST-1 mesh were stacked to form SCS, the conversion rate was 25% and the selectivity was close to 100% under COH condition. Under the MWI method, the VAL conversion rate and selectivity could reach to 100%. The results suggested that SCS was definitely capable of converting VAL to VN with high selectivity and yield, while MWI could effectively improve the conversion rate of VAL. The MWI was more favorable than COH because MWI provided a more efficient heating process with rapid and intense heating from the interior of catalyst. These Cu–O groups of HKUST-1 could absorb microwave, which made it more effective for VAL conversion. Secondly, benzene-1,3,5-tricarboxylic acid ligands (BTC ligands) also absorbed microwave and promoted the catalytic activity of Cu–O groups. On the other hand, CC was validated as a powerful microwave collector, rapidly receiving heat from the interior at MWI.

The synergistic effect of multiple metal active sites contributed to the cleavage of C–C and C–O bonds. Liu et al. synthesized a novel mixed valence POM-based MOF catalyst, $[\text{Cu}^{\text{I}}(\text{bbi})_2]_2\{[\text{Cu}^{\text{I}}(\text{bbi})]_2\text{V}^{\text{IV}}_2\text{V}^{\text{V}}_8\text{O}_{26}\}\cdot 2\text{H}_2\text{O}$ (NENU-MV-5, bbi = 1,1'-(1,4-butanediyl)bis(imidazole)) (Figure 4A). As a heterogeneous catalyst without any co-catalysts, NENU-MV-5 effectively catalyzed the one-step oxidative cleavage of β -O-4 lignin to phenols and aromatic acids with high activity and selectivity under an oxygen atmosphere.^[118] The catalysts showed good generality for the oxidative cleavage of a

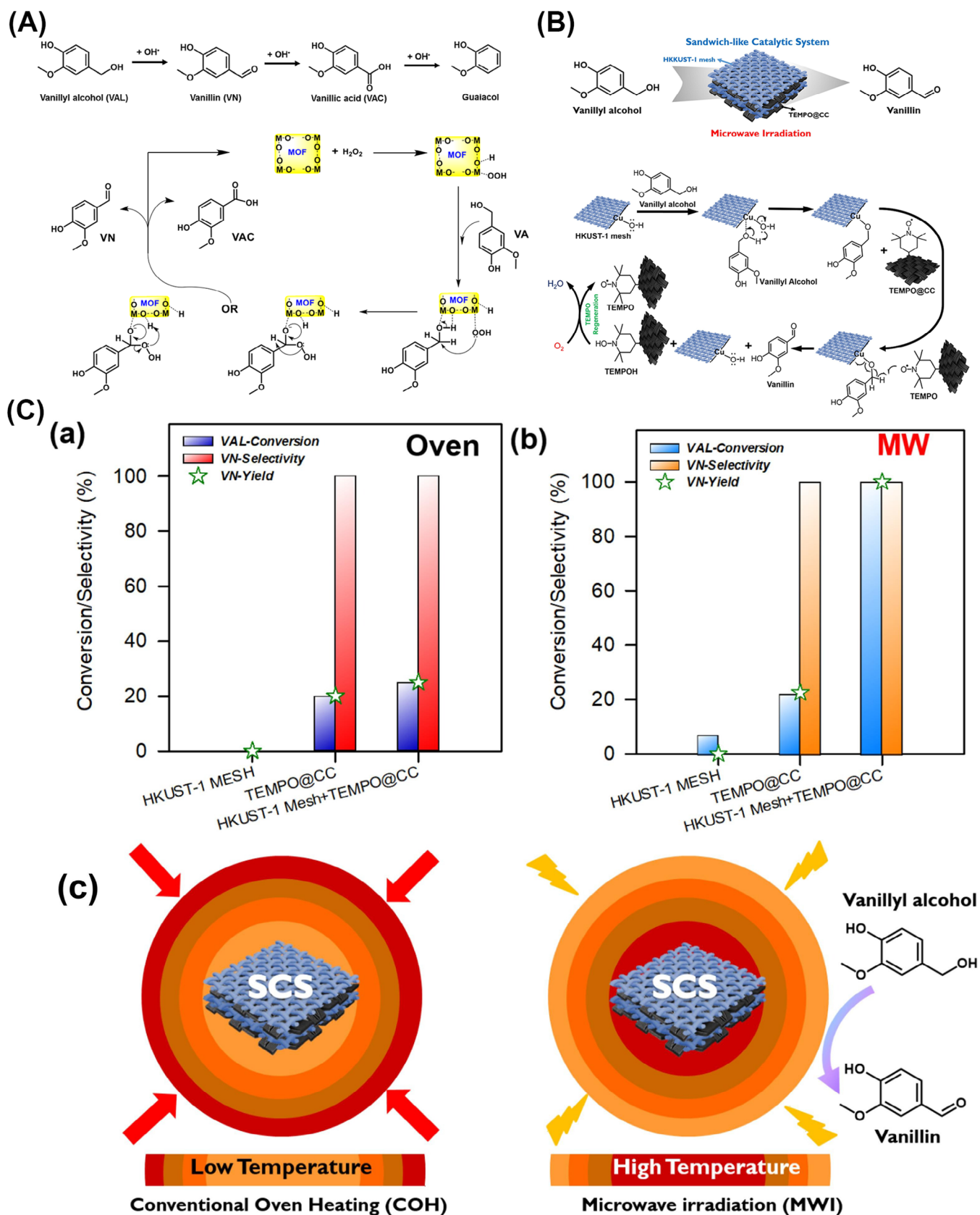


FIGURE 3 (A) Plausible mechanisms for oxidation of vanillyl alcohol (VAL) using metal-organic frameworks (MOFs) in the presence of H₂O₂ (OH[•]-based reaction and non-OH[•] reaction). Reproduced with permission: Copyright 2018, Springer Nature.^[117] (B) Schematic illustrations for preparation of HKUST-1 mesh via the one-step electrochemical synthesis and TEMPO@CC. (C) Conversion of VAL to vanillin (VN) using different materials (a) in a conventional oven and (b) under microwave irradiation; (c) temperature region distribution under the two distinct heating methods. Reproduced with permission: Copyright 2018, Elsevier.^[132]

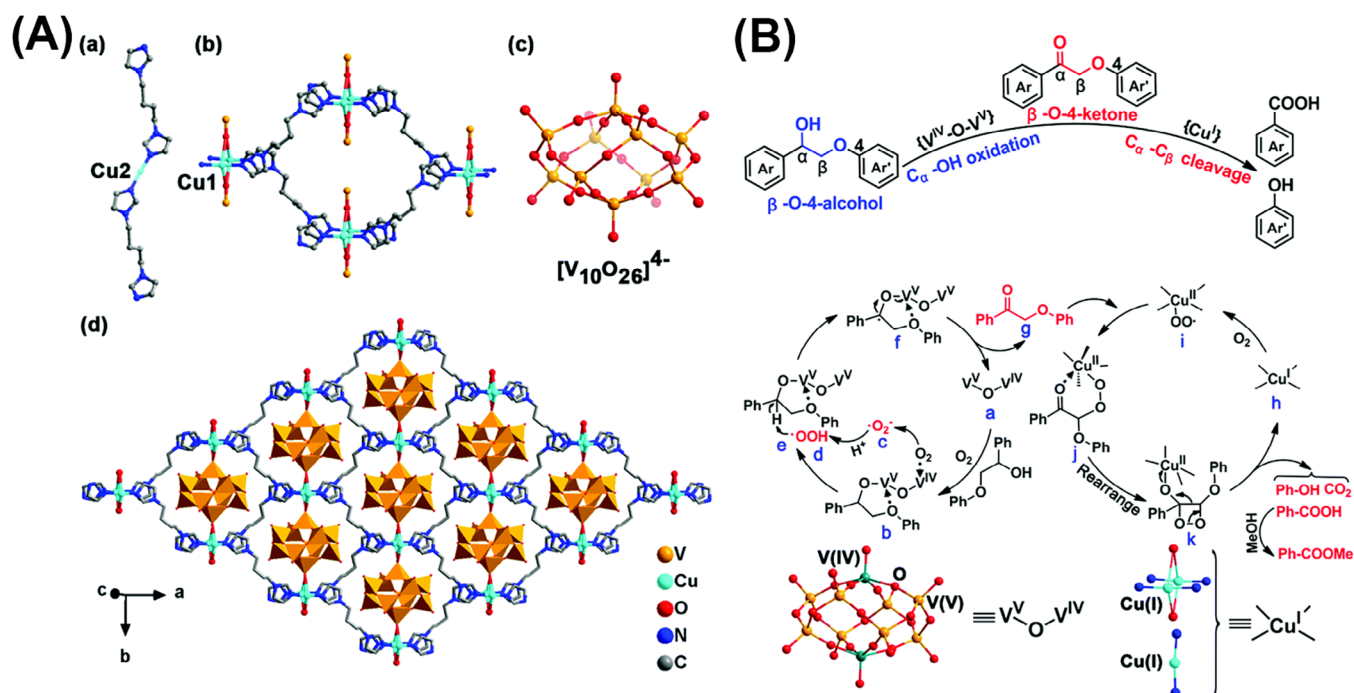


FIGURE 4 (A) Coordination mode of Cu2 (a), Cu1 (b), and $[\text{V}_{10}\text{O}_{26}]^{4-}$ (c); (d) 2D layer of $\{[\text{Cu}(\text{bbi})_2]_2\text{V}_{10}\text{O}_{26}\}^{2-}$. (B) Proposed catalytic mechanism of NENU-MV-5. Reproduced with permission: Copyright 2020, Royal Society of Chemistry.^[118]

series of β -O-4 lignin model compounds with methoxy and $\text{C}_\gamma\text{-OH}$ groups, achieving conversion rate of up to 99% and methyl benzoate yields of over 90%. The excellent catalytic performance of NENU-MV-5 could be attributed to the synergistic effect of multiple active sites. This process involved two steps (Figure 4B): β -O-4 alcohol was catalytically oxidized to β -O-4 ketone by the $\text{V}^{\text{V}}\text{-O-V}^{\text{IV}}$ dual site in the POM, and then Cu(I) active site rapidly cleaves of the $\text{C}_\alpha\text{-C}_\beta$ bond in β -O-4 ketone. Electron paramagnetic resonance (EPR) experiments, control experiments, and mechanistic studies were conducted to elucidate the specific catalytic mechanism. In both steps, molecular oxygen was essential. The $\text{V}^{\text{V}}\text{-O-V}^{\text{IV}}$ moiety could also catalyze the oxidation of 1-phenyl-2-phenoxyethanol to 2-phenoxy-1-phenylethanone. This might be attributed to the activation of O_2 to $\cdot\text{O}_2^-$ by the Lewis acidity of V(IV) and the activation of the $\text{C}_\alpha\text{-H}$ bond by V(V) interaction with 1-phenyl-2-phenoxyethanol. The resulting $\cdot\text{O}_2^-$ combined with H^+ from MeOH to form $\text{HOO}\cdot$, which abstracted a H atom from C_α to rapidly form 2-phenoxy-1-phenylethanone. In the Cu(I)-catalyzed oxidative cleavage of 2-phenoxy-1-phenylethanone, Cu(I) interacted with O_2 to generate $\text{Cu}(\text{II})\text{-OO}\cdot$, and then catalyzed the $\text{C}_\alpha\text{-C}_\beta$ bond cleavage of 2-phenoxy-1-phenylethanone to yield benzoic acid and phenol formate. Subsequently, the latter underwent decarboxylation to produce phenol and CO_2 (Figure 4B). Methyl benzoate was formed through esterification of benzoic acid with MeOH.

2.2 | Conversion of lignin, its model compounds, and derivatives by MOF composites

The cleavage of aryl ether bonds ($\text{C}_{\text{aryl}}\text{-O}$ and $\text{C}_{\text{alkyl}}\text{-O}$) in the lignin structure is an important mean to promote value-added chemicals and fuels.^[122] However, when the

ether linkage in lignin was broken, general hydrogenation reduction might cause the aromatic compounds to be simultaneously hydrogenated, thereby losing their aromaticity.^[136] Metal NPs have been widely reported as redox active sites for efficient conversion of lignin-related substances. MOFs have become a promising heterogeneous catalyst material due to their high specific surface area, adjustable pore size, and inherent host-guest chemistry.^[137] Although MOFs can be used as substrates to composite with various substances, research on catalytic conversion of lignin has mainly focused on the loading of metal NPs due to efficient conversion of metal NPs. Metal NPs can be stably immobilized or confined in unsaturated sites or pores of MOFs, thus reducing NP leakage.^[136]

Loading metal NPs in MOFs not only increased the active sites of the assembled MOF composites, but also enhanced the activity of synergistic catalysis. Furthermore, functionalization of organic ligands, metal-oxygen clusters, and overall frameworks and further hybridization with metal NPs would help to improve the activity of the composite catalysts. The synergistic effect between metal NPs and MOFs promoted the performance of catalysts.^[138] Zaheer and coworkers used a dual-solvent method to prepare the Pd@MOF catalyst, achieving uniform distribution of Pd NPs into the pores of MIL-101-Cr MOF.^[139] This catalyst achieved complete oxidative reduction of the C-O bond in β -O-4 lignin model compounds without the use of any base or external hydrogen source. Among them, the catalytic performance reached its optimal effect in a mixed solvent of ethanol and water: the conversion rate could reach 99%, and the yield could also reach more than 99%. The good hydrothermal stability and Lewis acidity of MIL-101-Cr promoted the cleavage of O-H bonds.^[140,141] Then, Pd NPs in the MOF catalyzed the dehydrogenation of $\text{C}_\alpha\text{-OH}$ bonds by self-hydrogen transfer to cleave $\text{C}_\beta\text{-O}$ bonds, thereby avoiding the use of any external hydrogen source. Pd NPs effectively adsorbed the H

in lignin model compound to form Pd–H species, and then broke the C–O bond through self-hydrogen transfer to obtain the target product. The strategy of fixing metal Pd NPs on MOFs not only successfully prepared recyclable heterogeneous catalysts but also improved the catalytic effect through the synergistic advantages of MOFs and Pd NPs. Srivastava and coworkers also reported a similar strategy aimed at finding a MOF-based catalyst with optimal bonding to aryl ethers and their hydrogenation products to achieve good catalytic activity and recyclability.^[136] In their study, a Pd NP-modified Ce-BTC MOF (Pd/Ce-BTC) was synthesized for the selective hydrogenation of benzyl phenyl ether (BPE) under mild temperature and pressure conditions. The study clearly elaborated the adsorption and catalytic mechanism. BPE was adsorbed on Ce-BTC, and H₂ was adsorbed and dissociated at the Pd site. Then, a hydrogen atom was transferred to the adsorbed BPE to produce toluene and phenol. Toluene was released and diffused, while phenol bound to the original adsorption site. Finally, phenol was desorbed, and the catalytic site was regenerated to continue adsorbing and catalyzing the cleavage of BPE. Under the same reaction conditions, the activity of Pd (1.5%) NP-modified Ce-BTC was twice that of Pd NP-modified CeO₂. The author provided a more in-depth explanation through X-ray photoelectron spectroscopy and density functional theory (DFT) calculations. There were more Pd⁰ in Pd/Ce-BTC, leading to more Pd–H sites available for hydrogenation. In addition, one of the hydrogenation products, phenol, had adsorption energies of –0.89 and –1.34 eV on the catalyst surface, forming more stable complexes with Pd/CeO₂, making it more difficult for the product to be desorbed and released, which is why the yield of the Pd/CeO₂ catalyst was lower than that of Pd/Ce-BTC catalyst. Third, the BPE substrate molecule had a higher adsorption energy on Pd/Ce-BTC, while phenol product had a lower adsorption energy on Pd/Ce-BTC, which was the main reason for the higher activity of Pd/Ce-BTC compared with Pd/CeO₂.

Traditional catalytic hydrogenolysis requires harsh conditions and excess hydrogen. It can be a safer, milder, and more valuable strategy of using hydrogen as donors or self-hydrogen transferring to replace H₂. POMs exhibit strong Brønsted acidity and redox activity, facilitating the transfer of H from the solvent to reactants. Zhang et al. prepared three-dimensional hierarchical flower-like bimetallic nitride nanosheets (SiW₁₂@Pd/Co-ZIF-NS) according to POM as a precursor to composite with Pd/Co-ZIF.^[142] Without additional H₂, the SiW₁₂@Pd/Co-ZIF-NS catalysts could break the C–O bond in phenyl ethers (β -O-4 model lignin dimers) selectively to produce ethylbenzene (87% yield) and phenol (93% yield) in isopropanol solvent, resulting from the synergistic action of acid and metal sites. Meanwhile, the catalyst also decomposed the model compound (4-benzyloxy-3-methoxybenzaldehyde) to the corresponding monomers: benzene, toluene, VN, GAL, and 2-methoxy-4-methylphenol. The catalysts also converted the more complex substances of 1-(3,4-dimethoxyphenyl)-2-(2-methoxyphenoxy) propane-1,3-diol to the products of arene, propylene, and o-hydroxyanisole with the yields of 66%, 31%, and 82%. This complex catalytic process underwent a tandem reaction of hydrogenolysis and HDO. Furthermore, it was inspiring to see that the conversion performance of the actual eucalyptus kraft lignin reached above 99%. The

total yield of the product monomer (41 wt%) approached to the complete cracking yield of the ether (45%–50%). Such superior efficiency might be owing to the porous hierarchical layer, the O-rich vacancy, and the cooperation of the active components. The reaction mechanism could be summarized as follows: the reactive (H*) in the hydroxyl group of isopropanol experienced the processes of adsorbing on and then spilling from the surface of Pd; the H⁺ from the Brønsted acid site and reactive H* were transferred to the electron-rich O and the electron-deficient N. Finally, the Pd–H species reduced the phenyl-Brønsted acid species to produce the corresponding aromatic compounds.

Uneven loading of metal catalytic sites complicates the revelation of active catalysts and reaction mechanisms. Therefore, it is highly desirable to design catalysts with uniformly distributed sites to improve the catalytic efficiency of lignin depolymerization and to understand C–O cleavage. Lin et al. introduced NiBr₂ into the Ti₈(μ_2 -O)₈(μ_2 -OH)₄ cluster of MIL-125 and further hydrogenated it to obtain Ni^{II} hydrogenation-modified MIL-125 catalyst (Ti^{III}₂Ti^{IV}₆-BDC-NiH) (Figure 5A,B).^[143] Under the conditions of no strong base added (1 bar H₂, 140°C, 6 h), the Ti₈-BDC-NiH catalyst selectively cracked the lignin model compounds containing α -O-4, β -O-4, and 4-O-5 bonds to generate hydrocarbons (aromatic hydrocarbon and cycloalkane) and alcohol compounds (aromatic alcohols and cyclohexanol). As shown in Figure 5C, DFT calculations revealed that the [Ni]–H catalyst first reacted with BPE through a four-center transition state, which involved [2 σ –2 σ] cycloaddition between [Ni]–H bond and “PhO–CH₂Ph” bond to generate [Ni]–OPh and toluene. [Ni]–OPh then reacted with H₂ through a four-center transition state along with σ -bond metathesis, yielding phenol and regenerating [Ni]–H to complete the catalytic cycle. The rate-determining step is the σ -bond metathesis between [Ni]–OPh and H₂. It was worth noting that once metal–oxygen cluster was further hydrogenated with NaBEt₃H, the electrons overflowed from Ni to Ti resulting in partial reduction of the Ti-oxo node on the cluster. Ti^{III}₂Ti^{IV}₆-BDC-NiH catalyst exhibited excellent activity for conversion of lignin model compounds, while Ti^{IV}₈-BDC-Ni^{II}-H was completely inactive, which also certified that the reduction of Ti₈ nodes was critical for the catalysis of the loaded Ni^{II}-H part. Unfortunately, the synergetic effect of the two metals need further comparative explications from the aspects of the catalyst effects of MIL-125, the activation energy barrier of single Ti, as well as the energy barrier of Ni and Ti synergistic effects.

Lignin derivatives were widely applied in recent studies. For example, VN, 4-methoxyphenol, ferulic acid, and VAC were referred to as lignin-like pyrolysis oil.^[132,134,144] These compounds were mainly linked by ether bonds, making deoxygenation difficult.^[145] Adopting similar strategies, metal NPs fixed in the MOFs could provide high-activity catalytic sites for HDO reaction of the aforementioned lignin derivatives.^[35,111,114,146]

The stable MIL-101 was used to encapsulate Pd NPs, which also showed good performance in the HDO reaction of lignin derivatives. Xu et al. fixed Pd NPs in the mesoporous MIL-101 to prepare Pd@MIL-101 catalysts (Figure 6A). Under mild reaction conditions using water as a green solvent, this catalyst exhibited high activity and selectivity for the HDO of VN to 2-methoxy-4-methylphenol (Figure 6B).^[111] The high activity and selectivity were

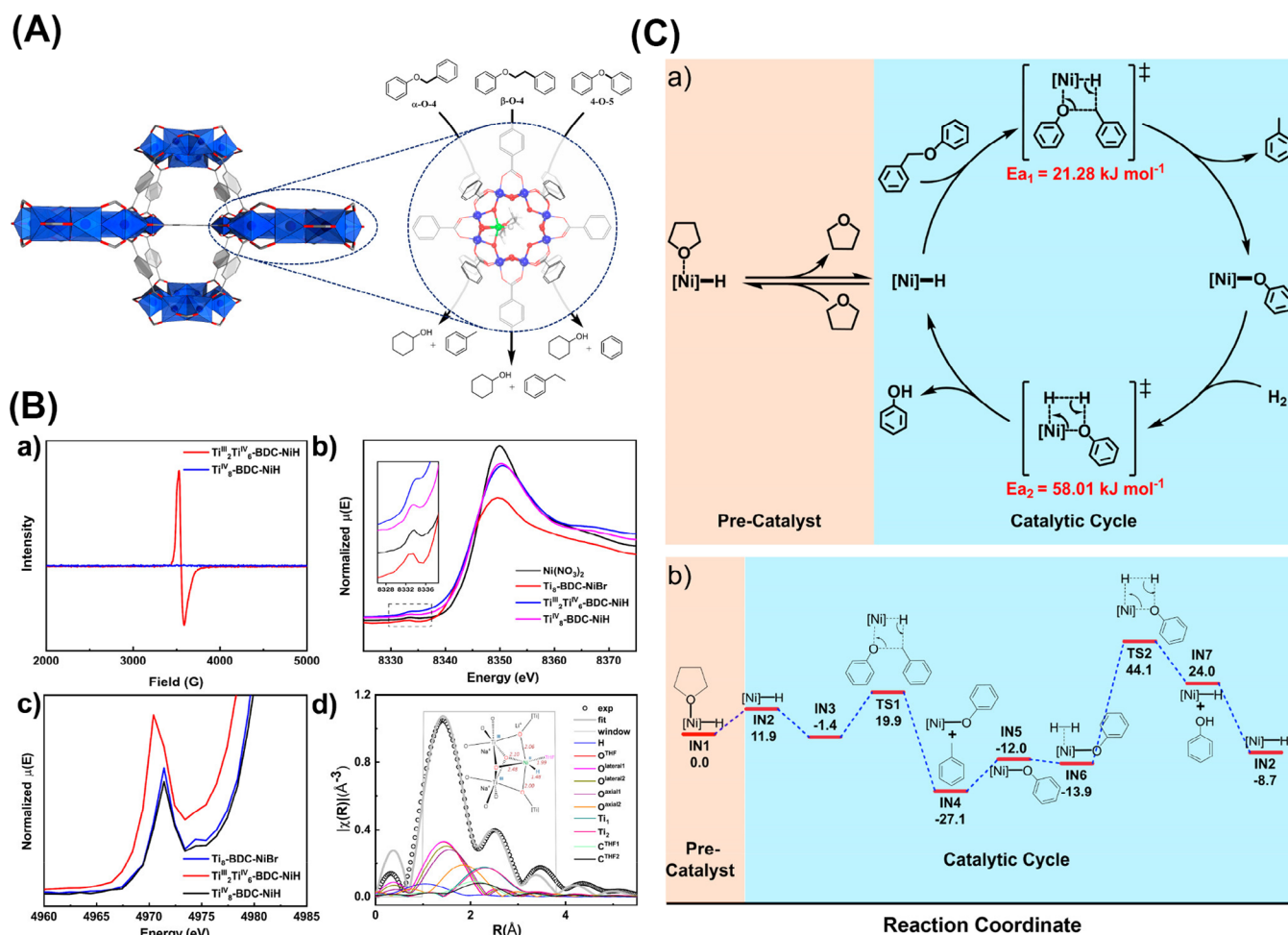


FIGURE 5 (A) Ti₈ node-supported Ni^{II}-H-catalyzed hydrogenolysis of lignin model compounds; titanium, nickel, oxygen, carbon, and hydrogen atoms shown in blue, green, red, gray, and white, respectively. (B) EPR spectra, Ni K-edge X-ray absorption near edge structure (XANES) spectra, Ti K-edge XANES spectra, and extended X-ray absorption fine structure (EXAFS) spectra of Ti^{IV}₈-BDC-NiH. (C) (a) Proposed mechanism for the hydrogenolysis of benzyl phenyl ether (BPE) (α-O-4) by the Ti^{IV}₈-BDC-NiH, and (b) density functional theory (DFT)-computed minimum-energy reaction path diagram for the catalytic hydrogenolysis on the Ni-H site. Reproduced with permission: Copyright 2019, American Chemical Society.^[143]

mainly attributed to the nanoconfinement effects, strong interactions between the reactants and catalysts, and small Pd NPs. Previous studies reported^[35,37,147,148] that close contact between metal and Brønsted acid sites could accelerate the HDO process. Owing to the higher oxophilicity of Hf(IV), Hf-based MOFs containing the μ₃-OH groups exhibited strong Brønsted acidity.^[149,150] Inspired by this, Kalidindi and coworkers prepared a Pd@UiO-66(Hf) core-shell catalyst to convert VN into 2-methoxy-4-methylphenol through the HDO reaction (Figure 6C).^[114] The excellent catalytic activity and selectivity of Pd@UiO-66(Hf) were attributed to the synergistic effect between Pd and μ₃-OH. Pd@UiO-66(Hf) core-shell catalyst outperformed Pd/UiO-66(Hf) support catalyst and physical mixture (Figure 6D). At 90°C, the conversion of VN reached 99%, with a selectivity for 2-methoxy-4-methylphenol of 99%. The Pd@UiO-66(Hf) catalyst could maintain at least five cycles, and the hot filtration test also confirmed the stability of the catalyst (Figure 6E). The possible mechanism was that H⁺ attacked the -OH group, leading to the cleavage of alkyl-OH bonds through water elimination. Subsequently, the intermediate interacted with the hydrogen atoms on Pd to produce 2-methoxy-4-methylphenol.

By modifying organic ligands, metal oxo clusters, and whole frameworks, the structure and function of MOFs could

be modulated. Mild conditions using water as a green solvent required precise regulation of hydrophilicity/hydrophobicity of MOF catalyst. Considering the hydrophilic nature of the reactant VN, Ma and coworkers attempted to adjust the wettability of the MOF carrier to precisely design metal catalyst performance. They introduced sulfonic acid groups into the MIL-101 framework and dispersed Pd NPs into the MOF framework to produce the superhydrophilic Pd/MIL-101-SO₃Na catalyst for VN conversion.^[146] Notably, the catalytic performance of Pd/MIL-101-SO₃Na significantly exceeded that of the pristine MIL-101 and Pd/C catalysts. First, the presence of hydrophilic reactants and intermediates increased contact opportunities between the catalyst and reactants/intermediates, thereby enhancing reaction efficiency. Second, the adsorption of hydrophobic products (2-methoxy-4-methylphenol) on the catalyst surface was reduced, avoiding clogging of active sites. Therefore, superhydrophilic Pd/MIL-101-SO₃Na exhibited excellent conversion rate (about 100%) and selectivity (about 100%). Introduction of amino groups into MOFs not only increased their hydrophilicity but also facilitated the formation of leaching resistant, uniform, and well-dispersed Pd NPs throughout the MOF framework. El-Shall and coworkers encapsulated Pd NPs (1.5–2.5 nm) in the NH₂-UiO-66 framework through direct anion exchange and H₂ reduction.^[35] The 2.0 wt%

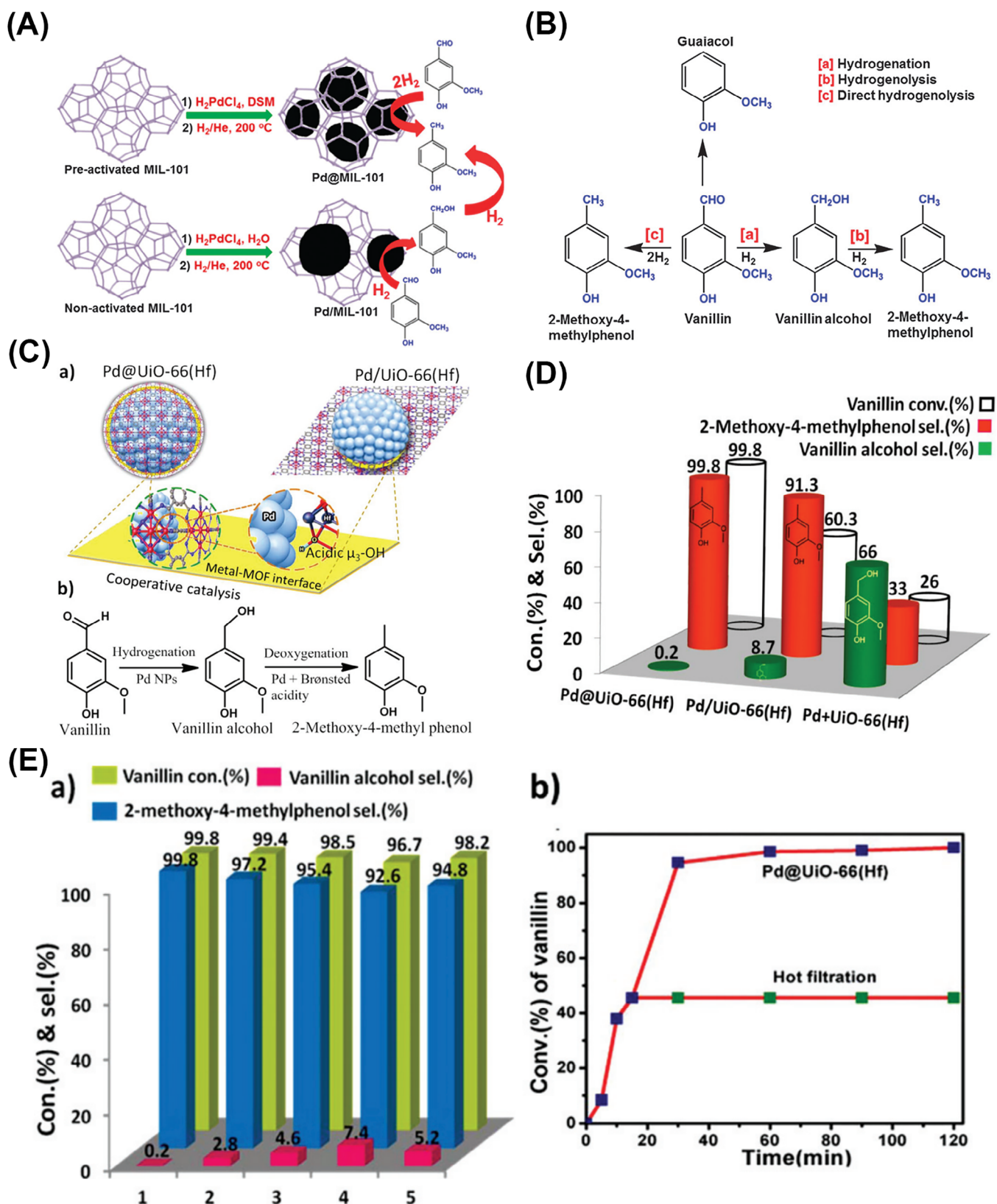


FIGURE 6 (A) Schematic representation of the immobilization of Pd nanoparticles into/onto MIL-101, and their use for catalytic hydrodeoxygenation (HDO) reactions of vanillin (VN). (B) Possible reaction pathways for VN HDO. Reproduced with permission: Copyright 2015, Royal Society of Chemistry.^[111] (C) Schematic representation of the Pd@UiO-66(Hf) core-shell and Pd/UiO-66(Hf) materials, and VN HDO reaction steps. (D) Comparison between the catalytic performances: conversion and product selectivity for VN HDO over the Pd@UiO-66(Hf) core-shell, Pd/UiO-66(Hf) support, and the Pd⁺ UiO-66(Hf) physical mixture. (E) Recyclability of the Pd@UiO-66(Hf) catalyst and hot filtration test for the Pd@UiO-66(Hf) catalyst. Reproduced with permission: Copyright 2019, Royal Society of Chemistry.^[114]

Pd@NH₂-UiO-66 catalyst completely transformed VN into 2-methoxy-4-methylphenol at 0.2 MPa H₂ and 75°C, with 100% conversion and selectivity. The synergistic catalysis between the MOF host and metal NP guests resulted in excellent catalytic performance in the VN HDO reaction. The MOF framework facilitated the transformation of the intermediate, while the Pd NPs effectively performed hydrogenolysis reduction. The authors emphasized the key role of the free amine moiety in the formation of leaching-resistant, uniform, and well-dispersed Pd NPs within the Pd@NH₂-UiO-66 framework. However, there was a lack of testing and discussion of the catalytic performance of Pd-loaded UiO-66 framework to illustrate the role of amino groups. Overall, functionalized MOFs have opened up a new avenue for improving the good dispersion and synergistic catalytic performance of metal NPs.^[35,136,146]

Defect engineering has been shown to be a novel tailoring strategy for improving catalytic activity. The introduction of ligand-unsaturated defects in MOFs leads to the creation of unsaturated metal sites that can be used as Lewis acid sites for various reactions. At the same time, defects in MOFs missing ligand linkages can be used to create additional centers of catalytic activity. Using defective MOFs as carriers to composite metal NPs is an excellent strategy to improve catalytic activity. Wang et al. prepared defect-engineered NH₂-MIL-53(Al) (abbreviated as NH₂-MIL-53-d) via trifluoroacetic acid modulation and loaded it with Pd NPs to obtain a bifunctional catalyst (Pd/NH₂-MIL-53-d) (Figure 7A).^[151] Proper use of trifluoroacetic acid to partially replace the NH₂-BDC ligand introduced defects and generated unsaturated metal sites. Furthermore, the unsaturated sites served as anchoring points for the uniform dispersion of Pd NPs on the MOF framework. The Pd/NH₂-MIL-53-d catalyst was used for the catalytic conversion of VN. A systematic study on the effects of reaction temperature, hydrogen pressure, and time was conducted (Figure 7B). Under low H₂ pressure (1 bar), VN and eight other lignin derivatives were completely transformed into decarbonylation products with a yield of over 99% at 120°C within 1 h. The non-defective ordinary Pd/NH₂-MIL-53 catalyst also achieved 100% conversion but maintained a selectivity of 94%–100%. The high catalytic performance of Pd/NH₂-MIL-53-d was attributed to the synergistic effect between the Pd NPs and the defects in the MOF structure. DFT calculations were conducted for the entire reaction mechanism (Figure 7C), including two parts: (i) hydrogenation of VN to VAL, and (ii) hydrogenolysis of VAL to 2-methoxy-4-methylphenol (MMP). VN HDO reaction began with the adsorption of VN and four H* species on the Pd site. Then, H* reacted with the –CHO group to form IM1, which underwent hydrogenation to form IM2. IM2 was unstable and could be desorbed from the Pd site as an intermediate product (4-hydroxy-3-methoxybenzylalcohol, HMP). Subsequently, the C–O bond in the hydroxymethyl group of HMP was broken, which in turn generated MMP by undergoing HDO. C₇H₇O₂CH₂* and OH* adsorbed on the Pd site to form IM3, which then underwent hydrogenolysis to generate the target product MMP. Notably, the rate-limiting step was the dehydrogenation of HMP due to the higher activation energy for this reaction compared with that of hydrogenation of VN. Additionally, the complete hydrogenation product (MMP) was much more thermodynamically stable than the partial hydrogenation product (HMP). The

synergistic effect between the Lewis acid sites and the highly dispersed Pd NPs was a key determinant of efficient HDO catalysis (Figure 7D). While this study reported excellent catalytic performance for the catalyst, it lacked comparisons among NH₂-MIL-53, defect-engineered NH₂-MIL-53, and Pd-loaded NH₂-MIL-53 for catalytic experiments. Analysis of these comparisons would help further elucidate the independent and synergistic effects of MOF frameworks, defects, and NPs on VN conversion rate and selectivity.

2.3 | Conversion of lignin, its model compounds, and derivatives by MOF-derived materials

In addition to pristine MOFs and MOF composites, MOF-derived catalysts with metal/metal oxide-doped N/C prepared from MOF have been widely developed. This process usually involves the redox of metals and carbonization of organic ligands by pyrolysis. Compared with the pristine MOFs and MOF composites, the MOF-derived catalysts exhibit higher thermal and chemical stability. At the same time, MOF-derived catalysts still retain some advantages of MOFs: the morphology, size, and metal site of catalysts can be designed and tailored by modulating the type of MOF precursor and carbonization conditions. MOF-derived catalysts are also emerging in the study of catalytic conversion of lignin-related substances due to these advantages.

Ni-MOF-derived materials were active in the catalytic conversion of lignin derivatives. Liao and coworkers synthesized novel Ni-MOF and further calcined it at 700°C to prepare a MOF-derived catalyst (Ni-MFC-700).^[152] The catalyst was able to efficiently convert VN into MMP in methanol at 160°C and 2 MPa H₂ with 100% conversion and 96.5% selectivity. The conversion of aldehyde group (–CHO) to methyl (–CH₃) was effectively promoted through reductive etherification and hydrogenolysis of C–O ether bonds in methanol. In addition, the catalytic process could be controlled for the directed production of methyl ether. Similarly to the material, Cao et al. synthesized a Ni/N–C catalyst by pyrolysis using a Ni-MOF as the feedstock (Figure 8A).^[153] The catalytic hydrogenolysis performance of this catalyst for C–O bonds cleavage was evaluated using diphenyl ether as a model compound. The catalyst completely converted diphenyl ether to monomers (benzene, cyclohexanol, and cyclohexane) by cleavage of the C_{aromatic}–O bond with a selectivity of 99.1%. It is worth noting that relatively low H₂ pressure is crucial for improving the monomer selectivity. However, H₂ is relatively hazardous when used as an H source for catalytic hydrogenolysis. Liu et al. prepared the Ni@C-650 catalyst to efficiently depolymerize lignin and its derivatives by utilizing isopropanol solvent as an in situ hydrogen source (Figure 8B).^[17] This work avoided the use of externally H₂ as the H source and utilized the solvent itself as the H source, which was greener and safer. The degradation efficiency of BPE reached over 90.2% when the reaction temperature was above 150°C (Figure 8B). In addition, Ni@C-X also showed a better applicability to the depolymerization reaction of lignin in practical applications. 4-Ethyl-phenol and 4-ethyl-2-methoxy-phenol were obtained in yields of 4.16 and 3.41 wt%, respectively. The catalyst was able to successfully break the β-O-4, β–β bond, and

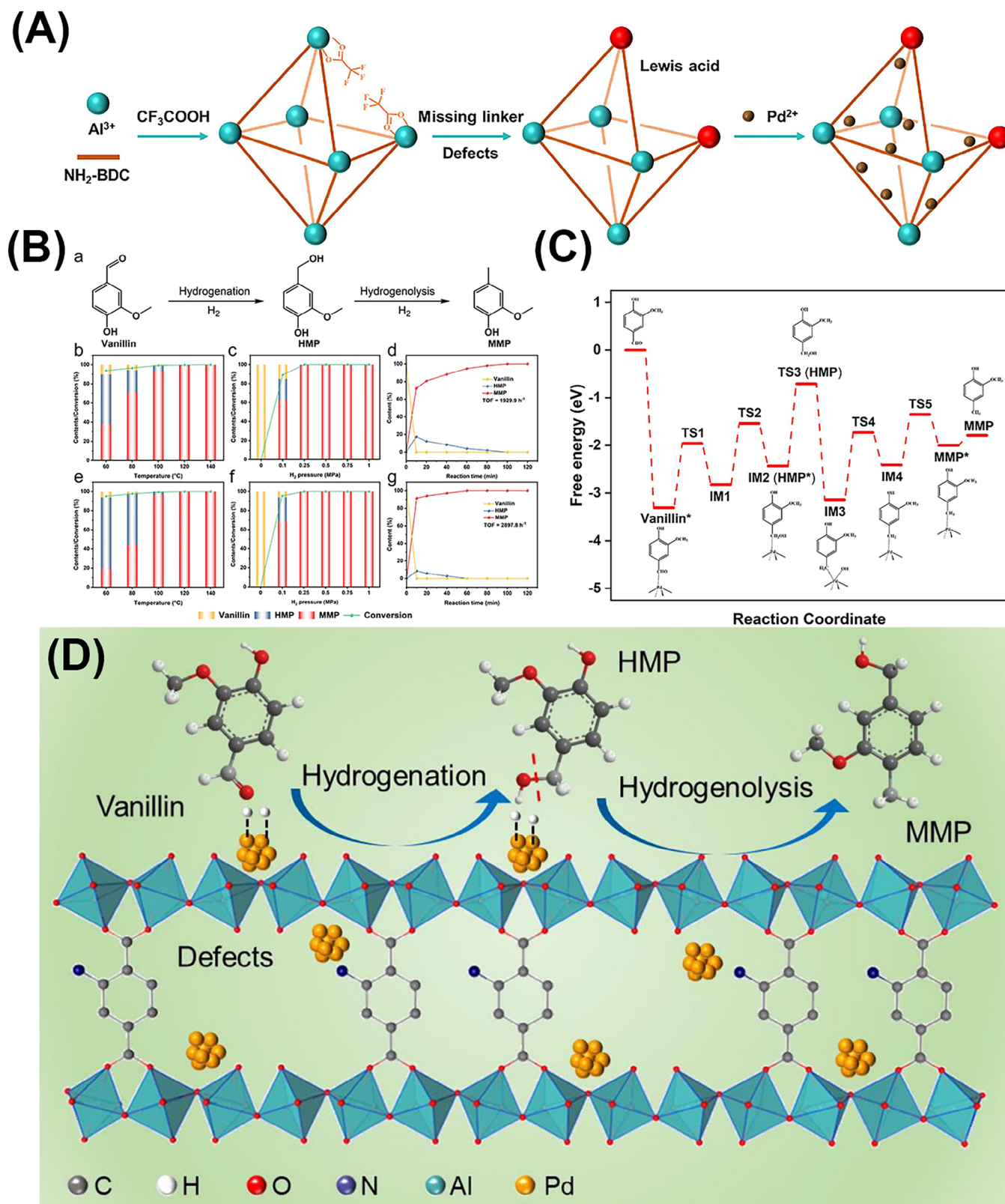


FIGURE 7 (A) Schematic synthetic route of Pd/NH₂-MIL-53-d. (B) The reaction pathway of vanillin (VN) hydrodeoxygenation (HDO) conversion into MMP over Pd/NH₂-MIL-53 and Pd/NH₂-MIL-53-d in water (a); effect of reaction temperature (b), H₂ pressure (c), and time (d) on VN conversion over Pd/NH₂-MIL-53; effect of reaction temperature (e), H₂ pressure (f), and time (g) on VN HDO over Pd/NH₂-MIL-53-d. (C) Energy profile of the hydrogenation of VN to MMP over the defective NH₂-MIL-53 supported Pd₄ cluster catalyst. (D) Pd/NH₂-MIL-53-d for VN HDO conversion. Reproduced with permission: Copyright 2023, Elsevier.^[151]

α -O-4 bond in the lignin structure, and selective deoxygenation of lignin was realized without any initial reaction pressure (Figure 8C). Figure 8D summarizes the possible reaction pathways for lignin depolymerization involving with dealkylation, demethoxylation (DMO), and decarbonylation.

In addition to the excellent catalytic properties of Ni-based MOF derivatives, there were Mo-based MOF materials that have shown some effects in the HDO of GAL.^[154–156] For example, although MoC could cleave aromatic carbon–oxygen (C_{aryl}–O) and alkyl carbon–oxygen (C_{alkyl}–O) in

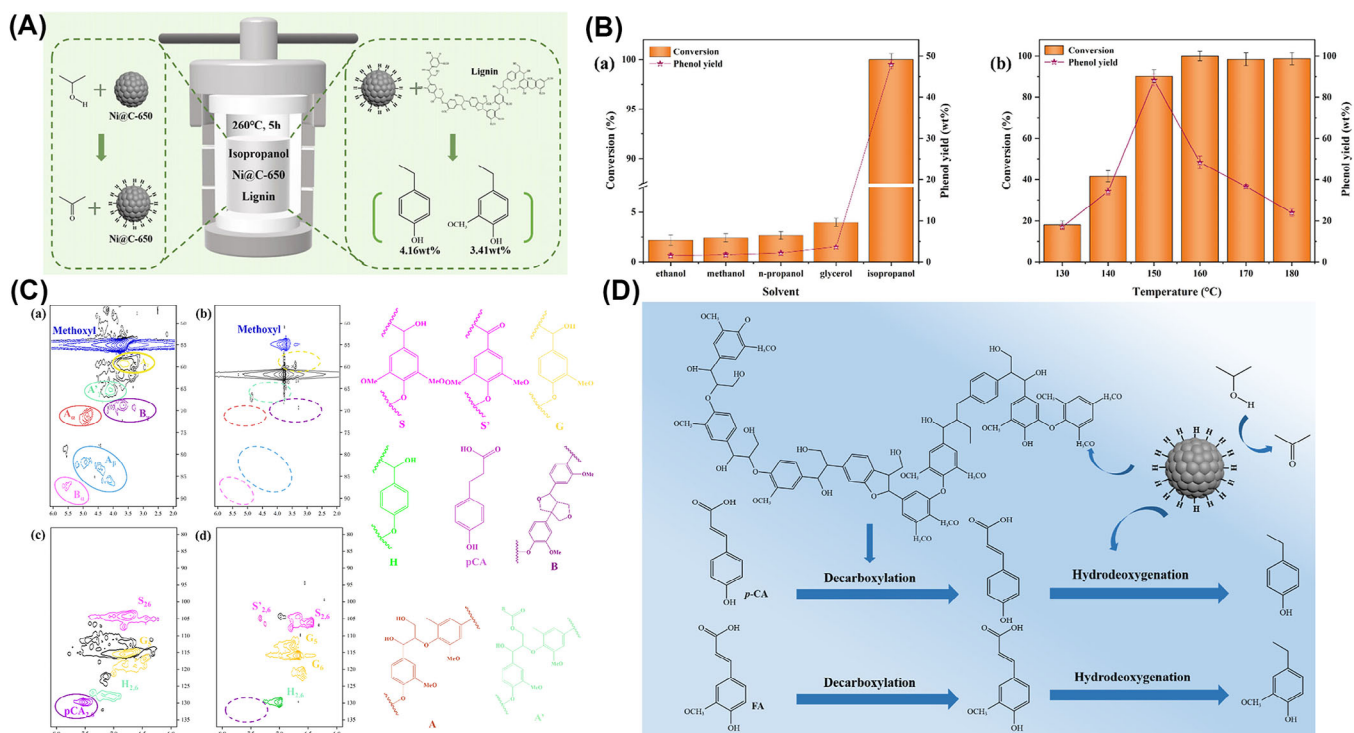


FIGURE 8 (A) Scheme of Ni@C-650 synthesis and hydrodeoxygenation (HDO) of lignin derivatives. (B) Effect of reaction solvent and temperature. (C) 2D-HSQC NMR spectra of lignin and bio-oil: (a) aliphatic regions of lignin, (b) aromatic regions of lignin, (c) aliphatic regions of the bio-oil, and (d) aromatic regions of the bio-oil. (D) Possible reaction pathways for lignin depolymerization. Reproduced with permission: Copyright 2022, American Chemical Society.^[17]

lignin and lignin model compounds, the selectivity of its target product, phenol, had yet to be improved. In order to improve the phenol selectivity, Zhu and coworkers synthesized a series of one-dimensional N-doped molybdenum carbide materials (N-Mo₂C@C-T) by calcining Mo-MOF via “pyrolysis-carbothermal reduction” process. N-Mo₂C@C-T catalyst was used for the catalytic conversion of aryl ethers and enzymatically solubilized lignin (Figure 9A,B).^[122] β-O-4, α-O-4/β-5, and β-β linkages were decreased due to the attack during catalytic cracking process, indicating that N-Mo₂C@C-700 exhibited good activity on C–O bond cleavage (Figure 9C). With appropriate Mo⁵⁺ content, N-Mo₂C@C-700 showed the highest catalytic activity and selectivity for phenol in the cleavage of C_{aryl}–O bonds in diphenyl ethers. The underlying reason for the difference in catalytic activity was the formation of N-Mo₂C by insertion of various amounts of N through suitable carbonization temperature. The N component acted as an electron acceptor and thus affected the valence and surface property of the Mo active center.

Co-MOF-derived materials exhibited excellent performance in the catalytic oxidation of GAL. Zhou and coworkers prepared a series of Co/C-n-x-T catalysts using MOFs and lignin under calcination conditions (n: lignin species; x: lignin content; T: calcination temperature).^[157] The catalytic activity of different Co/C-n-x-T catalysts for lignin-derived bio-oil (GAL) was investigated by using isopropanol solvent as the hydrogen proton source to instead of hydrogen gas. The conversion rates and products were investigated under different lignin contents, different reaction temperature, reaction time, and initial nitrogen pressure. Among them, Co/C-EL-0.5-5-500 showed the best catalytic activity, with 100% conversion rate of GAL and up to 90%

yield of cyclohexanol under the optimal conditions of 240°C, 0 MPa N₂, and 4 h (Figure 10A–D). The high catalytic activity was mainly attributed to the large specific surface area, good dispersibility, small Co particle size, and optimal acidity. GAL is a typical lignin model compound containing C_{aryl}–OH, C_{aryl}–OCH₃, and C_{aryl}O–CH₃ and an aromatic ring in its molecular structure. Different reaction pathways existed during hydrotreating process of GAL, such as hydrogenation, demethylation, DMO, and direct dehydration.^[158] Based on previous research, two competing reaction pathways existed in converting GAL into cyclohexanol (Figure 10C): (i) GAL underwent aromatic ring hydrogenation to produce 2-methoxycyclohexanol, followed by DMO to produce cyclohexanol (pathway III); and (ii) GAL was first converted to phenol by DMO, followed by phenol hydrogenation to produce cyclohexanol (pathway I). At the same time, there was a side reaction (pathway II). The research work involved methoxycyclohexanol in pathway III, 1-methyl-1,2-cyclohexanediol in pathway II, and 2-hexanone and 2-hexanol in pathway I. In this work, HDO of GAL involved different competing reactions and different products. Unfortunately, the mechanism of this research work needs to be further investigated.

The introduction of other suitable metal ions into single-metal MOF-based catalysts can help to further improve the catalytic activity in biomass depolymerization.^[10] Such bimetallic catalysts exhibited excellent catalytic activity and selectivity in biomass energy conversion.^[159,160] Zhou et al. prepared a series of Ni_xMo_y@C catalysts (Figure 11A) by calcining a series of bimetallic MOF-derived materials (NiMo MOFs) for the conversion of lignin monomers, dimers, trimers, and actual lignin for the production of chemicals and liquid fuels with high hydrogen-to-carbon ratio

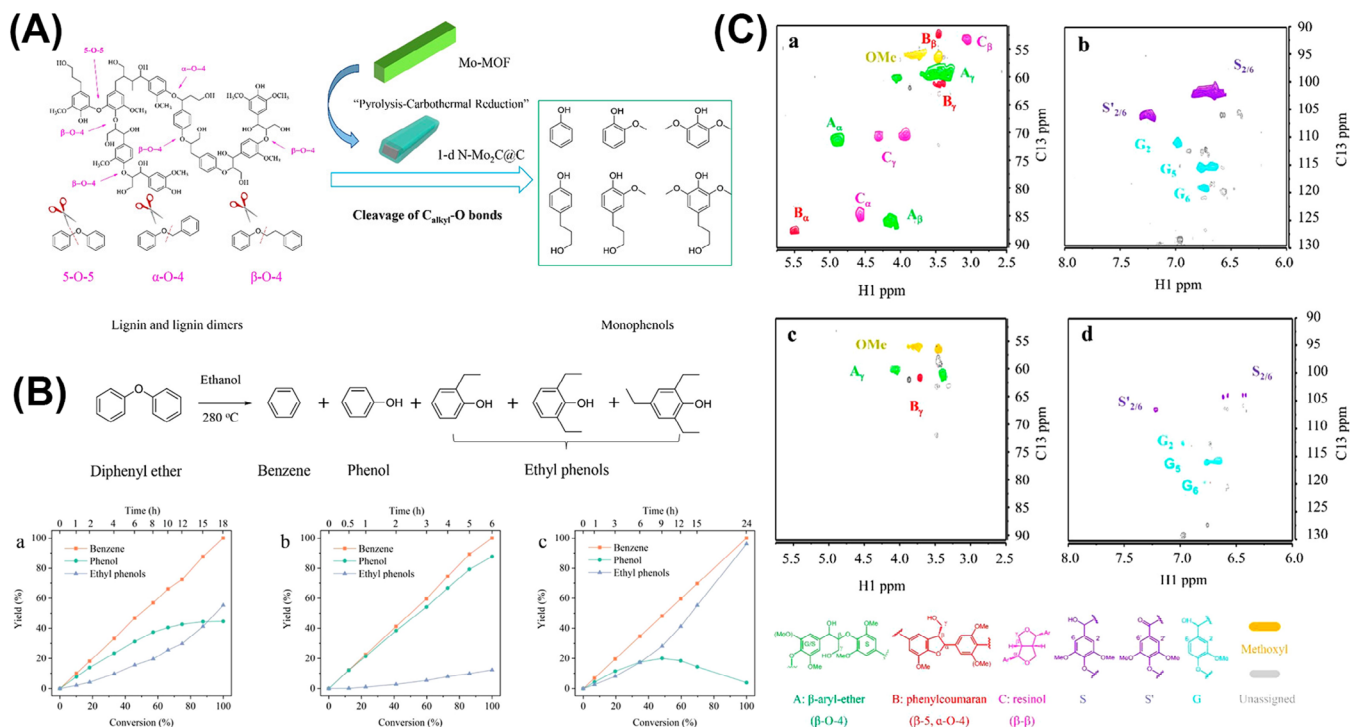


FIGURE 9 (A) Ni-MOF-mediated synthesis of one-dimensional nitrogen-doped molybdenum carbide for the cleavage of lignin and dimeric lignin model compounds. (B) Product distribution as a function of diphenyl ether conversion over N-Mo₂C@C-T catalysts: (a) N-Mo₂C@C-650, (b) N-Mo₂C@C-700, and (c) N-Mo₂C@C-750. (C) 2D-HSQC NMR spectra of raw lignin (a and b) and liquid products (c and d) obtained from lignin depolymerization. Reproduced with permission: Copyright 2020, American Chemical Society.^[122] MOF, metal-organic framework.

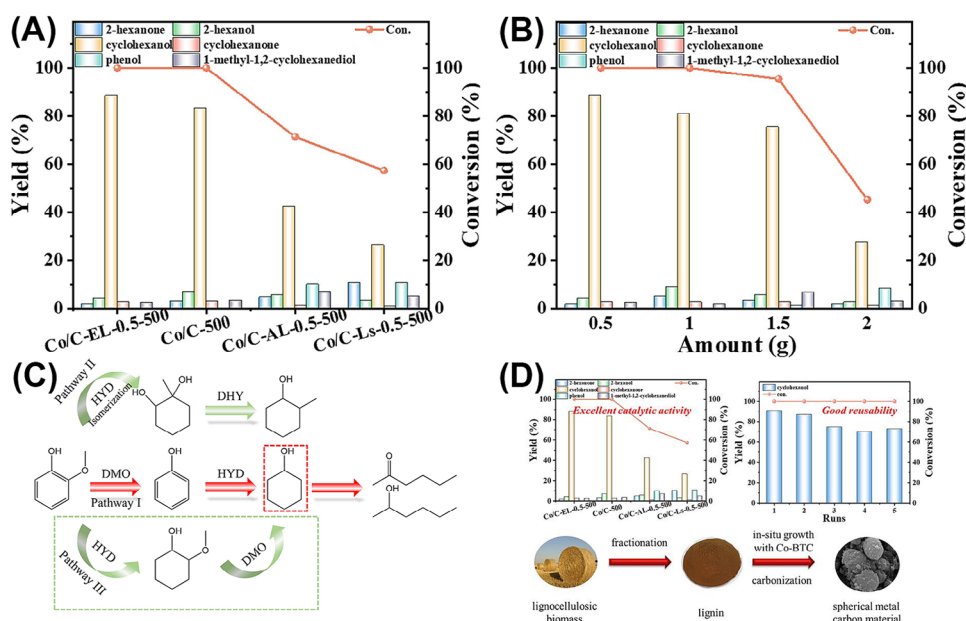


FIGURE 10 (A) Performance evaluation of different catalysts in guaiacol (GAL) conversion to cyclohexanol: the effect of different lignin varieties. (B) Effect of enzymatic lignin amount on GAL conversion and product distribution. (C) Possible reaction pathways in the hydrogenation of GAL to cyclohexanol over Co/C-EL-0.5-500. Green dotted box: reaction pathway in other's research. Red dotted box: main product. (D) Lignin-derived metal carbon material for the catalytic hydrotreatment of GAL to cyclohexanol. Reproduced with permission: Copyright 2023, Elsevier.^[157]

(H/Ceff) values. Based on the optimal reaction conditions (Figure 11B), the Ni₄Mo₁@C catalyst converted 2-phenoxy-1-phenylethan-1-ol to ethylcyclohexane and cyclohexanol in yields of 95% and 92%, respectively, which were much higher than that of the Ni@C catalyst without the introduction of metal Mo. The incorporation of Mo reduced the particle size of the spherical catalyst, enhanced the electron

transfer between metal Mo and Ni, and improved the acid strength. The Ni₄Mo₁@C catalyst exhibited excellent HDO catalytic activity due to the enhanced hydrogenation activity by the synergistic effect of Mo and Ni (Figure 11C). Given the demanding reaction conditions (240°C, 4 h, 2 MPa H₂), there is a further need to explore high (H/Ceff) chemicals under mild conditions to achieve higher yields of realistic

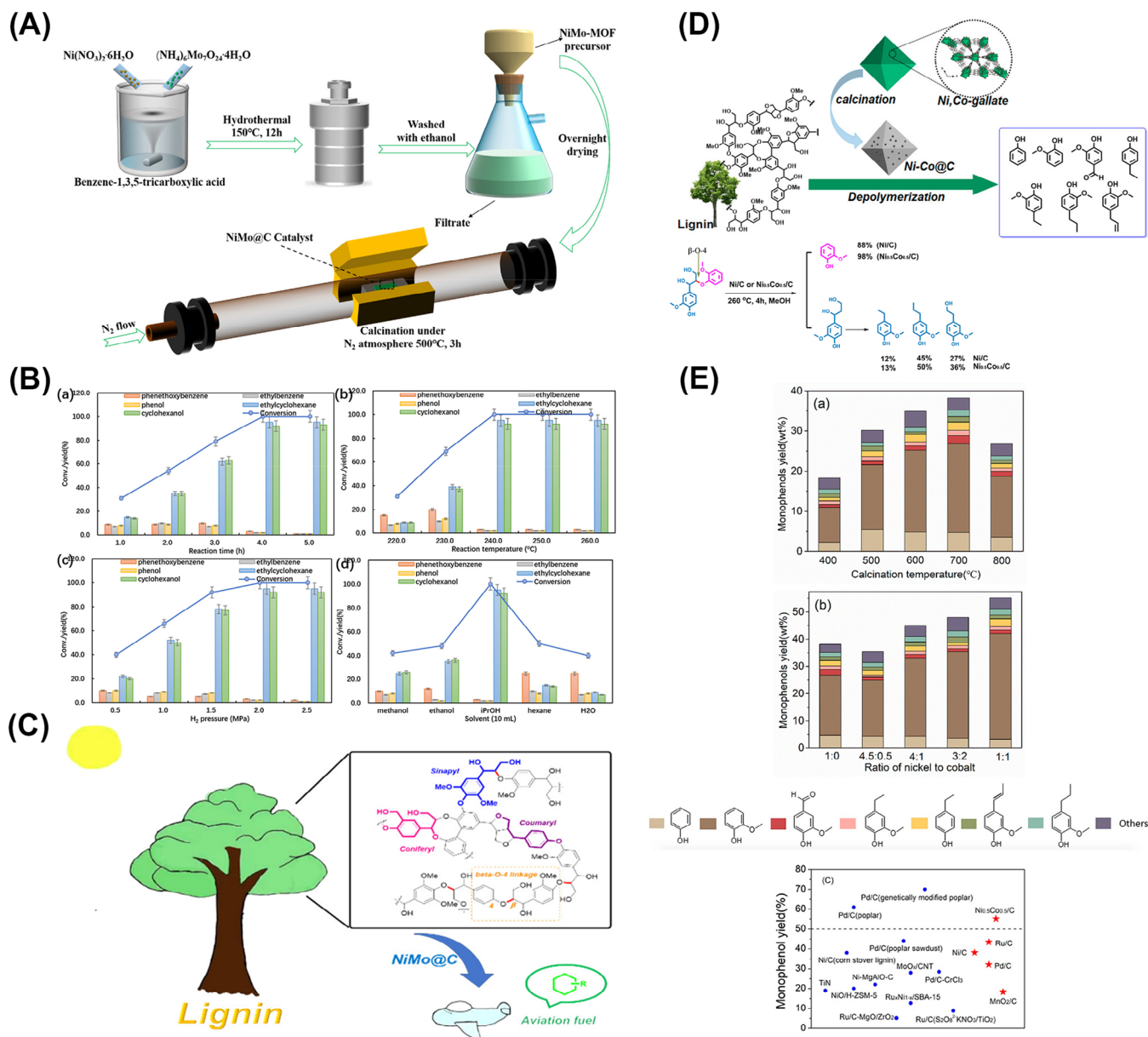


FIGURE 11 (A) Detailed preparation process of the desired catalyst. (B) Hydrotreatment of the β -O-4 lignin dimer over the $\text{Ni}_4\text{Mo}_1\text{@C}$ catalyst: (a) effect of reaction time, (b) effect of reaction temperature, (c) effect of H_2 pressure, and (d) effect of solvents. (C) Catalytic conversion of lignin to liquid fuels with an improved H/Ceff value over bimetallic NiMo-MOF-derived catalysts. Reproduced with permission: Copyright 2021, American Chemical Society.^[10] (D) Schematic diagram of Ni-Co/C synthesis, and depolymerization path of guaiacylglycerol- β -guaiacyl ether (GG) on Ni/C and $\text{Ni}_{0.5}\text{Co}_{0.5}\text{/C}$ catalyst. (E) Catalytic activity measurements: (a) monophenol yield on Ni/C catalyst with different calcination temperatures, (b) monophenol yield on $\text{Ni}_x\text{Co}_{1-x}\text{/C}$ catalyst, (c) monophenol yield on different catalyst. Blue circles represent materials reported in the literature, and red pentagrams represent materials prepared in this work. Reproduced with permission: Copyright 2019, American Chemical Society.^[123] MOF, metal-organic framework.

lignin. Zhou et al. prepared monometallic Ni@C and bimetallic NiLa@C materials for the catalytic hydrogenolysis of lignin dimers to cycloalkanes/cyclohexanols using Ni-MOF and NiLa-MOF.^[161] Different C–O bonds in the lignin dimer were cleaved, followed by further hydrogenation to give the products cycloalkanes (jet fuel) and cyclohexanol. The bimetallic NiLa@C catalyst not only exhibited synergistic effects but also displayed uniform dispersion, increased total acidity and improved Brønsted acid/Lewis acid ratio (B/L) relative to the Ni@C catalyst. This resulted in higher catalytic activity during C–O bond breaking and subsequent hydrogenation/HDO reactions. In addition, the simulation study showed that the mixture could be readily separated into two fine chemicals (cycloalkanes and cyclohexanol in this paper) at atmospheric pressure, with cyclohexanol having

a purity as high as 99.5%. This study might provide a new pathway for the value added of lignin-derived dimers and provide inspiration for the production of more biomass fuels and fine chemicals (e.g., cycloalkanes, cyclohexanols, etc.).

Similar work involved the formation of bimetallic alloys with Co and Ni. The catalysts exerted bimetallic synergistic effects to improve catalytic performance. Ren and coworkers utilized gallate-based MOFs as precursors to prepare the monometallic catalyst and bimetallic catalyst (Ni/C and Ni-Co/C). These catalysts were used for converting poplar lignin to monophenols (Figure 11D).^[123] The effects of Ni/C catalyst with preparation temperature and the effects of $\text{Ni}_x\text{Co}_{1-x}\text{/C}$ catalyst with different nickel/cobalt atomic ratios were investigated and optimized (Figure 11E). The optimized catalyst ($\text{Ni}_{0.5}\text{Co}_{0.5}\text{/C}$) prepared at 700°C. With

methanol as the solvent, the $\text{Ni}_{0.5}\text{Co}_{0.5}/\text{C}$ catalyst catalyzed guaiacylglycerol- β -guaiacyl ether (GG) to produce monophenols. The total yield of monophenols was 55.2% and GAL selectivity could be as high as 70.3%, which exceeded most of the top-performing catalysts. GG as the model compound of the lignin was used to explore the reaction mechanism. For both Ni/C and $\text{Ni}_{0.5}\text{Co}_{0.5}/\text{C}$ catalyst, GAL was the main product due to the cleavage of the β -O-4 bond, and the others were ethyl guaiacol, propyl guaiacol, and pinacol. This showed that the β -O-4 bond could be broken selectively (Figure 11D). The conversion rate of GG was 83.5% based on Ni/C catalyst, while the $\text{Ni}_{0.5}\text{Co}_{0.5}/\text{C}$ catalyst exhibited better conversion rate of GG (97.5%). Compared with the Ni/C catalyst, the addition of Co greatly improved the performance of the catalyst. The reason for this might be that cobalt enhanced the HDO activity.^[132] In addition, Co and Ni could form an alloy structure, which might produce a synergistic effect. Cyclohexane and its derivative products were not detected throughout the reaction, indicating that the benzene ring was not over-hydrogenated. The Ni/C and $\text{Ni-Co}/\text{C}$ catalysts were able to select for the depolymerization of the lignin model compound (GG), where the β -O-4 bond was selectively broken and the benzene ring was not over-hydrogenated. This study provided a reference model for catalysts in the selective degradation of lignin to aromatic hydrocarbon compounds.

3 | CONVERSION OF LIGNIN, ITS MODEL COMPOUNDS, AND DERIVATIVES BY COF-BASED MATERIALS

COFs as a new class of highly crystalline porous organic materials are usually constructed by reversible condensation reactions between organic monomers. Several characteristics of COFs can be designed and adjusted (e.g., components, pore sizes, morphologies, etc.) according to the demands of catalytic conversion of lignin-related substances. Their porous nature provides more opportunities for the adsorption of reactants. The intrinsic and external active components can promote the activated cleavage of lignin-related substances. In addition, the inherent framework structures and the tunable components of COFs can be beneficial for the preparation of composites to improve the catalytic performance, such as surface modification, metal loading, etc. However, it is still in its infancy that applying the COF-based materials to conduct the catalytic conversion of lignin-related substances and a series of research will continuously advance the progress in this field.

3.1 | Conversion of lignin, its model compounds, and derivatives by pristine COFs

The structure of β -O-4 accounts for about 50% of all lignin junctions.^[162] It is crucial to convert lignin into aromatic compounds by fracturing β -O-4 bonds. Most of the homogeneous or heterogeneous catalysts that have been reported utilize metal active centers as the key to catalysis, such as transition metals (e.g., vanadium,^[163–166] copper,^[167] cobalt^[168]), precious metals (e.g., rhenium^[169] and palladium^[170]), etc. The use of cheaper metal-free catalysts has also aroused the interest of researchers to explore

catalytic conversion of lignin-related substances. Metal-free addition of graphene and ionic liquids as catalysts have successively been shown to be effective in the catalytic cleavage of lignin model compounds.^[171–173] The reaction mechanism and reaction pathway for the breaking of chemical bonds in lignin model compounds in metal-free catalytic systems remain unclear and unknown. In addition, the inherent difficulty of lignin cleavage reactions has led to limitations in the development of effective metal-free catalytic systems. The pristine COFs as a molecular catalyst have similar advantages to MOFs, such as highly ordered pore structure, tunable structure and function, etc. In addition, COFs with the highly ordered molecular structure provide the feasible platform to carry out studies on the catalytic mechanism of non-metallic materials. Therefore, pristine COFs have also attracted much attention as a novel metal-free material in the field of catalysis. The use of pristine COFs for the conversion of lignin-related substances will be beneficial to gain insight into the catalytic mechanism by metal-free materials, as well as provide more possibilities and guidance for the development of metal-free catalysts.

Xu and coworkers prepared a series of covalent triazine frameworks (CTFs) using different dinitrile monomers.^[11] With the participation of oxygen, the CTFs acted as metal-free catalysts to efficiently catalyze the cleavage of the lignin model compound (2-phenoxyacetophenone) to produce phenol, benzoic acid, methyl benzoate, and methyl benzoylformate. The conversion under optimal conditions could reach more than 99% and the selectivity of the cleavage products reached 92% when CTF-*p*-DCB-1 (*p*-DCB = 1,4-dicyanobenzene) was used as a catalyst. This research work systematically investigated the effect of different solvents on conversion of lignin model compound. When linear alcohols were utilized as solvents, similar conversion rates of about 80% were obtained along with high selectivity of the product. However, when utilizing non-protonic solvents, among them, the conversion could also be as high as more than 90% in cyclohexane and *N,N*-dimethylformamide, but the selectivities of the cracked products were both very low; and when acetonitrile and dimethylsulfoxide were used as solvents, the conversion rates and selectivities were very poor. Second, this work also explored the effect of oxygen atmosphere. On the one hand, the essentiality of oxygen atmosphere was confirmed by comparative experiments with N_2 . On the other hand, $^{18}\text{O}_2$ isotope tracer experiments confirmed that the O in benzoic acid was derived from oxygen and that of phenol from the reactant, as well as revealed that methyl benzoate was obtained by the reaction of benzoic acid and methanol. Most importantly, the work revealed the intermediates and reaction pathways of the catalytic conversion through free radical trapping experiments, deuterium-labeling experiments, and a series of mechanism investigations. The $\text{C}_\beta\text{-H}$ activation was the rate-determining step in the catalytic cleavage of the lignin model compound. $\text{C}_\beta\text{-H}$ bond was activated and inserted via O_2 to form a peroxide, which was shown to be involved in the catalytic oxidative cleavage of 2-phenoxyacetophenone. The phenylglyoxal and phenyl formate were obtained by cleavage of the $\text{C}_\beta\text{-O}$ and $\text{C}_\alpha\text{-C}_\beta$ bonds, which might be intermediates of the reaction, whereas methyl benzoylformate might not be an intermediate of the reaction. Ketone was likely to be an intermediate, but not a direct intermediate, forming a reversible equilibrium with

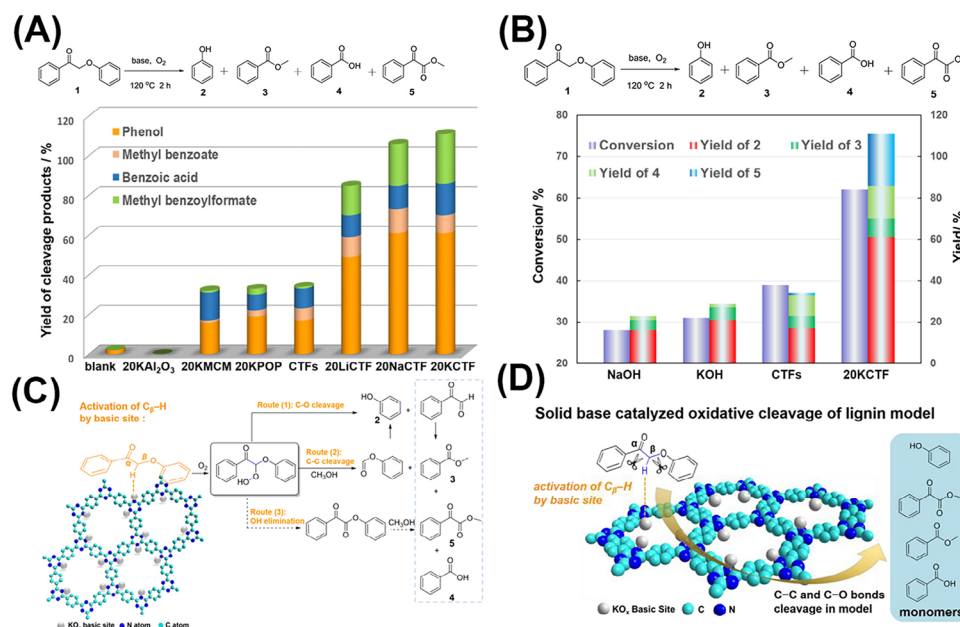


FIGURE 12 (A) Cleavage reaction of model 1 under various catalytic conditions. Other bases were studied by adding the same molar amount of alkaline metal as for the 20KCTF catalyst. (B) Effects of base on the cleavage reaction at 120°C. The NaOH and KOH reactions were conducted by adding the same molar amount of alkaline metal as that for the 20KCTF catalyst. (C) Proposed cleavage pathway for strong-base-promoted oxidative cleavage of 2-phenoxy-1-phenylethanone substrate. (D) Schematic diagram of strong-base-modified covalent triazine frameworks (CTFs) for lignin oxidative cleavage. Reproduced with permission: Copyright 2020, American Chemical Society.^[194]

the reaction substrate. The authors proposed a possible cleavage mechanism for the reaction. Initially, C_β-H was activated to produce peroxides, and the 2-phenoxyacetophenone could form a reversible equilibrium with ketone. Then, the peroxide was involved in the cleavage reaction of the C-C or C-O bond to produce phenyl formate and phenylglyoxal intermediates, respectively, along with phenol and benzoic acid products. CTFs catalyzed phenylglyoxal with methanol into benzoic acid, methyl benzoate, and benzoylformate, while releasing CO₂. Another pathway to methyl benzoate was through the slow esterification of benzoic acid.

3.2 | Conversion of lignin, its model compounds, and derivatives by COF composites

Increasing the cleavage rate of chemical bond under relatively mild conditions could reduce the re-polymerization of phenolic monomers to some extent, resulting in high yields of phenolic monomers.^[174–176] The activation of the C_β-H bond plays a key role in the oxidative/cleavage of β-O-4 bond in lignin-related substances.^[11,167,172,177] Introducing some reactive components in COFs may be a promising method to activate C_β-H bond cleavage. And, the development of catalysts capable of efficiently activating this bond will help to increase the conversion rate.

Surface alkalinity was an important factor affecting the catalytic process.^[178–180] It could facilitate a variety of reactions by activating O-H and N-H bonds, among others.^[181,182] Alkali could help to activate the C-H bond.^[183,184] However, studies on base-catalyzed depolymerization of lignin were performed under extremely harsh reaction conditions, usually at elevated temperatures above 270°C and accompanied by high pressures.^[175,185–188] Moreover, most of the studies were carried out to explore the effects on lignin cleavage with

the addition of alkali (e.g., NaOH or Cs₂CO₃, etc.).^[189–191] No attention was paid to the effect of catalyst surface alkalinity on C-H bond activation. Based on the previous CTF, Xu and coworkers synthesized potassium nitrate-modified CTF using a wet impregnation method. Subsequently, KCTF catalyst with basic sites (KO_x species) was prepared by calcination under the condition of maintaining the original porous skeleton.^[192] Compared with CTF catalyst, KCTF catalyzed the cleavage reaction of a lignin model compound (2-phenoxy-1-phenylpropionophenone) with significantly higher conversion and selectivity. The introduction of strong basic sites could effectively improve the cleavage ability of catalysts (Figure 12A). Other similar strong basic sites (LiO_x and NaO_x) were introduced to the CTF and showed similar promotion effects (Figure 12B). Further control experiments showed that the cleavage activity of CTF modified with strong alkaline site (20KCTF) was much higher than that of NaOH, KOH, and CTF (Figure 12B). In addition, the increase in the number of basic sites was accompanied by an increase in the catalytic activity. Among them, 30KCTF catalyst showed 95%–99% conversion rate in substrate extension experiments for derivatives of 2-phenoxy-1-phenylacetone. The KCTF-catalyzed lignin model compound mechanism is shown in Figure 12C,D, where in the first step, the strong basic sites on the CTF activated the C_β-H bond of the substrate and produce hydroperoxides in the presence of oxygen. The subsequent cleavage process might involve three main pathways (Figure 12C). (1) Hydroperoxides was converted to phenol and phenylglyoxal intermediate through C-O bond cleavage. Then, the phenylglyoxal intermediate was transformed to methyl benzoylformate, methyl benzoate, and benzoic acid. (2) C-C bond was fractured to produce the methyl benzoate product and the phenyl formate intermediate. The intermediate was converted to phenol. (3) In addition, base-catalyzed elimination of hydroxide leading to the formation of phenyl phenylglyoxylate might

be another route. This modification and composite strategy provided new insights into the design of catalysts for catalytic conversion of lignin-related substances.

Usually, bimetallic catalysts exhibit superior synergistic effects compared with monometallic catalysts. Au–Pd bimetallic catalysts can effectively break C–H bonds in toluene and methane, as well as catalytic conversion of a variety of different functional groups in biomass, including the catalytic conversion of alcohol groups and catalytic cleavage of C–C bonds. The introduction of bimetallic components into COFs is a promising strategy for catalytic cleavage of β -O-4 bonds. Xu and coworkers prepared Au–Pd–CTFs catalysts with different metal ratios using Au–Pd NPs to compound with CTFs, and then investigated the catalytic conversion efficiency of 2-phenoxy-1-phenylethanol.^[193] This work investigated the effect of different metal ratios and various carriers. The Au₁–Pd₁–CTF and Au₁–Pd_{1.5}–CTF catalysts exhibited the highest conversion (96%) and selectivity (91%) among all the Au–Pd–CTFs with different metal ratios. On the other hand, once replacing the CTFs carriers by other metal oxides, which resulted in much lower selectivity of the cracking products. The high performance of the Au–Pd–CTFs catalysts could be attributed to the following points. First, Au–Pd NPs could accelerate the activation of C–H bonds and further catalyze alcohol oxidation reactions. Second, the synergistic interactions between the Au–Pd NPs and the CTFs were necessary for the oxidative cleavage of the β -O-4 lignin model compounds. Last but not least, the framework structure of the CTFs provided high porosity and specific surface area to enhance mass diffusion.

4 | CONCLUSIONS AND PERSPECTIVES

Efficiently converting renewable lignin into valuable chemicals and fuels holds great significance in solving energy crisis and mitigating global warming. Based on the high specific surface area, controllable structure and pore, functionalized overall framework, and designable catalytic site, the rational design of MOF- and COF-based catalysts is a promising way to achieve conversion of lignin-related substances. Here, we reviewed the application of MOF- and COF-based materials in catalytic conversion of lignin-related substances. We introduced new strategies to enhance the activity of lignin conversion using MOF- and COF-based heterogeneous catalysts. Emphasis was placed on discussing and highlighting the catalytic mechanism in lignin-related substances as well as the structure–activity relationship of active centers. Although some progress has been made in this field, research on MOF- and COF-based catalysts for lignin conversion is still in its early stages and faces a number of challenges that need to be addressed.

For MOF-based materials, they are mainly divided into three categories: pristine crystalline MOFs, MOF composites, and MOF derivatives. Pristine crystalline MOF catalysts for lignin conversion have rarely been reported. More MOF catalysts with new structure need to be developed to reveal the mechanism of lignin catalytic conversion in order to establish the structure–performance relationship and further guide the design and synthesis of more new catalysts. In this process, advanced in situ characterization methods should be used to visualize the active sites and reaction pathways.

MOF composites as catalysts mainly focused on two aspects. First, loading precious metal NPs; second, ligands modification and further loading precious metal NPs. Currently, there is a lack of more functional modification of ligands and selection of composite material types. It is hoped that more functional ligands can be modified for different driving forces, solvents, and reaction substrates to assist the active sites in achieving catalytic reactions more efficiently. The loading of precious metals is usually used to improve the activity of catalysts. However, the scarcity and cost of precious metal materials limit their future industrial application. Replacing precious metals with abundant elements without changing the original catalytic activity is what we urgently hope to see. In addition, the preparation of composite materials using more types of materials and MOFs will also provide new options for achieving catalytic conversion of lignin-related substances. For MOF derivatives catalysts, most of them are obtained by controlling the pyrolysis of MOF. It is hoped that the types and catalytic effects of MOF derivatives can be optimized by adjusting the composition, structure, and morphology of MOFs materials. Second, through doping with multiple heteroatoms, the synergistic catalysis of MOF derivatives catalysts can be achieved to further regulate the activity and selectivity. Compared with pristine MOFs, these derived catalysts need more advanced in situ characterization techniques to systematically ascertain the complex active parts of the catalyst and explore the reaction pathway. At the same time, DFT theoretical calculations should be introduced and improved to assist in unveiling the catalytic mechanism of derived materials.

The application of COF materials in catalytic conversion of lignin-related substances is still in its infancy stage and needs further development. It is suggested that future research directions can focus on several aspects: (1) designing and synthesizing more COF-based materials are used for converting lignin-related substances to further optimize more efficient COF catalysts; (2) the structure and morphology of COFs may vary depending on different synthesis methods and reaction conditions, leading to different catalytic performances; (3) the catalytic mechanism of COF-based materials is still unclear, and it is urgent to clarify the active components and catalytic mechanism; (4) more efforts still need to be devoted to develop simple, low-cost, large-scale, high-yield materials, and synthesis strategies; (5) experimenting with different driving forces may modulate the catalytic performance, such as photocatalysis, thermal catalysis, electrocatalysis, photo-electrocatalysis, photo-thermal catalysis, etc.

There are also some challenges and opportunities in the catalytic reaction conditions of catalysts in the process of converting lignin-related substances with MOF- and COF-based materials. (1) Using alcohols and acids as hydrogen proton sources instead of hydrogen gas to achieve hydrogen transfer for catalytic reactions can reduce transportation, storage costs, and safety issues. Lignin itself contains rich hydroxyl groups that can be used as a source of protons. Therefore, designing an appropriate hydrogen transfer catalytic path can maximize atom utilization. Besides, the introduction of suitable hydrogen donor into MOF- and COF-based catalyst also provides a strategy to achieve this goal. (2) Water as a low-cost green solvent is promising for widespread use in the catalytic conversion of lignin-related substances.

Therefore, designing water-resistant porous catalysts for stable operation is crucial. Similarly, the stability against high temperatures, acids, bases, etc., also needs to be considered. (3) Pre-treating natural lignin with chemical methods (such as pre-oxidation) to weaken the hydrogen bonding energy in lignin and avoid re-polymerization is beneficial for subsequent conversion. (4) Most catalytic processes only achieve breaking C–O bond or simple HDO to obtain the products without C–C bond cleavage reaction because the C–C bonds with high dissociation energy are difficult to be attacked. This ultimately limits the type and quantity of monomers generated from lignin conversion. Designing efficient MOF- and COF-based catalysts with efficient catalytic systems for C–C and C–O bonds cleavage is expected to break the limitations on monomer production.

Finally, a deep insight of the relationship between the chemical/electronic/structural properties of MOF-/COF-based catalysts and their catalytic performance will be of great significance for the utilization of lignin. At the same time, it will be equally instructive for the development of a new generation of stable catalytic systems based on MOFs and COFs. If MOF- and COF-based catalysts can be developed for industrial catalytic conversion of lignin, it will be a milestone in the application of MOF- and COF-based catalysts in heterogeneous catalysis and biomass energy conversion.

ACKNOWLEDGMENTS

This work was financially supported by the National Natural Science Foundation of China (nos. 22101089, 22225109, 22175094, 21871141, 21871142, 22071109, and 92061101), the Guangdong Basic and Applied Basic Research Foundation (no. 2020A1515110836), and the Open Fund of Energy and Materials Chemistry Joint Laboratory of SCNU and TINCI (no. SCNU-TINCI-202204). Qing Huang and Pengfei Wu contributed equally to this work.

CONFLICT OF INTEREST STATEMENT

The authors declare they have no conflicts of interest.

ORCID

Ya-Qian Lan  <https://orcid.org/0000-0002-2140-7980>

REFERENCES

1. C. O. Tuck, E. Pérez, I. T. Horváth, R. A. Sheldon, M. Poliakoff, *Science* **2012**, 337, 695.
2. A. J. Ragauskas, G. T. Beckham, M. J. Biddy, R. Chandra, F. Chen, M. F. Davis, B. H. Davison, R. A. Dixon, P. Gilna, M. Keller, P. Langan, A. K. Naskar, J. N. Saddler, T. J. Tschaplinski, G. A. Tuskan, C. E. Wyman, *Science* **2014**, 344, 1246843.
3. Y. Shao, Q. Xia, L. Dong, X. Liu, X. Han, S. F. Parker, Y. Cheng, L. L. Daemen, A. J. Ramirez-Cuesta, S. Yang, Y. Wang, *Nat. Commun.* **2017**, 8, 16104.
4. R. Rinaldi, R. Jastrzebski, M. T. Clough, J. Ralph, M. Kennema, P. C. A. Bruijninx, B. M. Weckhuysen, *Angew. Chem. Int. Ed.* **2016**, 55, 8164.
5. H. Li, A. Bunrit, N. Li, F. Wang, *Chem. Soc. Rev.* **2020**, 49, 3748.
6. W. Schutyser, T. Renders, S. Van den Bosch, S. F. Koelewijn, G. T. Beckham, B. F. Sels, *Chem. Soc. Rev.* **2018**, 47, 852.
7. R. Fang, A. Dhakshinamoorthy, Y. Li, H. Garcia, *Chem. Soc. Rev.* **2020**, 49, 3638.
8. X. Wu, N. Luo, S. Xie, H. Zhang, Q. Zhang, F. Wang, Y. Wang, *Chem. Soc. Rev.* **2020**, 49, 6198.
9. C. Mondelli, G. Gözaydın, N. Yan, J. Pérez-Ramírez, *Chem. Soc. Rev.* **2020**, 49, 3764.
10. C. Chen, P. Liu, H. Xia, J. Jiang, X. Yang, M. Zhou, *ACS Sustain. Chem. Eng.* **2021**, 9, 13937.
11. L. Zhao, S. Shi, M. Liu, G. Zhu, M. Wang, W. Du, J. Gao, J. Xu, *Green Chem.* **2018**, 20, 1270.
12. G. E. Klinger, Y. Zhou, J. A. Foote, A. M. Wester, Y. Cui, M. Alherech, S. S. Stahl, J. E. Jackson, E. L. Hegg, *ChemSusChem* **2020**, 13, 4394.
13. J. R. Silverman, A. M. Danby, B. Subramaniam, *Reaction Chem. Eng.* **2019**, 4, 1421.
14. J. M. Nichols, L. M. Bishop, R. G. Bergman, J. A. Ellman, *J. Am. Chem. Soc.* **2010**, 132, 12554.
15. M. Graglia, N. Kanna, D. Esposito, *ChemBioEng Rev.* **2015**, 2, 377.
16. M. D. Kärkäs, B. S. Matsuura, T. M. Monos, G. Magallanes, C. R. J. Stephenson, *Org. Biomol. Chem.* **2016**, 14, 1853.
17. H. Li, M. Liu, W. Zou, Y. Lv, Y. Liu, L. Chen, *ACS Sustain. Chem. Eng.* **2022**, 10, 5430.
18. X. Zhang, M. Tu, M. G. Paice, *BioEnergy Res.* **2011**, 4, 246.
19. S. Contreras, A. R. Gaspar, A. Guerra, L. A. Lucia, D. S. Argyropoulos, *Biomacromolecules* **2008**, 9, 3362.
20. Y. Deng, X. Feng, M. Zhou, Y. Qian, H. Yu, X. Qiu, *Biomacromolecules* **2011**, 12, 1116.
21. R. Ma, M. Guo, X. Zhang, *Catal. Today* **2018**, 302, 50.
22. J. Luo, X. Zhang, J. Lu, J. Zhang, *ACS Catal.* **2017**, 7, 5062.
23. M. Gale, C. M. Cai, K. L. Gilliard-Abdul-Aziz, *ChemSusChem* **2020**, 13, 1947.
24. X.-M. Li, Y. Wang, Y. Mu, J. Gao, L. Zeng, *J. Mater. Chem. A* **2022**, 10, 18592.
25. T. Wei, Y. Zhou, C. Sun, X. Guo, S. Xu, D. Chen, Y. Tang, *Nano Res.* **2023**, <https://doi.org/10.1007/s12274-023-6187-8>.
26. T. Wei, J. Lu, P. Zhang, G. Yang, C. Sun, Y. Zhou, Q. Zhuang, Y. Tang, *Chin. Chem. Lett.* **2023**, 34, 107947.
27. X. Cen, Y. Sun, C. Yu, Z. Qiao, C. Zhong, *Aggregate* **2023**, 4, e361.
28. X.-M. Li, J. Gao, *SusMat* **2022**, 2, 504.
29. Y.-S. Xia, M. Tang, L. Zhang, J. Liu, C. Jiang, G.-K. Gao, L.-Z. Dong, L.-G. Xie, Y.-Q. Lan, *Nat. Commun.* **2022**, 13, 2964.
30. X. Zhang, Z. Wang, H. Jiang, H. Zeng, N. An, B. Liu, L. Sun, Z. Fan, *Sci. Adv.* **2023**, 9, eadh1415.
31. D. Yang, B. C. Gates, *ACS Catal.* **2019**, 9, 1779.
32. Q. Yang, Q. Xu, H.-L. Jiang, *Chem. Soc. Rev.* **2017**, 46, 4774.
33. M. Zhou, C. Tang, H. Xia, J. Li, J. Liu, J. Jiang, J. Zhao, X. Yang, C. Chen, *Fuel* **2022**, 320, 123993.
34. L. Lin, X. Han, B. Han, S. Yang, *Chem. Soc. Rev.* **2021**, 50, 11270.
35. F. Zhang, S. Zheng, Q. Xiao, Y. Zhong, W. Zhu, A. Lin, M. S. El-Shall, *Green Chem.* **2016**, 18, 2900.
36. Y.-Z. Chen, G. Cai, Y. Wang, Q. Xu, S.-H. Yu, H.-L. Jiang, *Green Chem.* **2016**, 18, 1212.
37. F. Zhang, Y. Jin, Y. Fu, Y. Zhong, W. Zhu, A. A. Ibrahim, M. S. El-Shall, *J. Mater. Chem. A* **2015**, 3, 17008.
38. K. T. Tan, S. Ghosh, Z. Wang, F. Wen, D. Rodríguez-San-Miguel, J. Feng, N. Huang, W. Wang, F. Zamora, X. Feng, A. Thomas, D. Jiang, *Nat. Rev. Methods Primers* **2023**, 3, 1.
39. S. Daliran, A. R. Oveisi, Y. Peng, A. López-Magano, M. Khajeh, R. Mas-Ballesté, J. Alemán, R. Luque, H. Garcia, *Chem. Soc. Rev.* **2022**, 51, 7810.
40. R. Liu, K. T. Tan, Y. Gong, Y. Chen, Z. Li, S. Xie, T. He, Z. Lu, H. Yang, D. Jiang, *Chem. Soc. Rev.* **2021**, 50, 120.
41. K. Geng, V. Arumugam, H. Xu, Y. Gao, D. Jiang, *Prog. Polym. Sci.* **2020**, 108, 101288.
42. W.-T. Chung, I. M. A. Mekhemer, M. G. Mohamed, A. M. Elewa, A. F. M. El-Mahdy, H.-H. Chou, S.-W. Kuo, K. C. W. Wu, *Coord. Chem. Rev.* **2023**, 483, 215066.
43. F. J. Uribe-Romo, C. J. Doonan, H. Furukawa, K. Oisaki, O. M. Yaghi, *J. Am. Chem. Soc.* **2011**, 133, 11478.
44. C. Qian, W. Zhou, J. Qiao, D. Wang, X. Li, W. L. Teo, X. Shi, H. Wu, J. Di, H. Wang, G. Liu, L. Gu, J. Liu, L. Feng, Y. Liu, S. Y. Quek, K. P. Loh, Y. Zhao, *J. Am. Chem. Soc.* **2020**, 142, 18138.
45. S.-Y. Ding, M. Dong, Y.-W. Wang, Y.-T. Chen, H.-Z. Wang, C.-Y. Su, W. Wang, *J. Am. Chem. Soc.* **2016**, 138, 3031.
46. S. Dalapati, S. Jin, J. Gao, Y. Xu, A. Nagai, D. Jiang, *J. Am. Chem. Soc.* **2013**, 135, 17310.
47. S. B. Alahakoon, C. M. Thompson, A. X. Nguyen, G. Occhialini, G. T. McCandless, R. A. Smaldone, *Chem. Commun.* **2016**, 52, 2843.
48. V. S. Vyas, F. Haase, L. Stegbauer, G. Savasci, F. Podjaski, C. Ochsenfeld, B. V. Lotsch, *Nat. Commun.* **2015**, 6, 8508.

49. Z. Li, Y. Zhi, X. Feng, X. Ding, Y. Zou, X. Liu, Y. Mu, *Chem. Eur. J.* **2015**, *21*, 12079.
50. Z. Li, X. Feng, Y. Zou, Y. Zhang, H. Xia, X. Liu, Y. Mu, *Chem. Commun.* **2014**, *50*, 13825.
51. Y. Li, C. Wang, S. Ma, H. Zhang, J. Ou, Y. Wei, M. Ye, *ACS Appl. Mater. Interfaces* **2019**, *11*, 11706.
52. G.-J. Chen, X.-B. Li, C.-C. Zhao, H.-C. Ma, J.-L. Kan, Y.-B. Xin, C.-X. Chen, Y.-B. Dong, *Inorg. Chem.* **2018**, *57*, 2678.
53. D. N. Bunck, W. R. Dichtel, *Chem. Eur. J.* **2013**, *19*, 818.
54. A. López-Magano, R. Mas-Ballesté, J. Alemán, *Adv. Sustain. Syst.* **2022**, *6*, 2100409.
55. I. Romero-Muñiz, A. Mavrandonakis, P. Albacete, A. Vega, V. Briois, F. Zamora, A. E. Platero-Prats, *Angew. Chem. Int. Ed.* **2020**, *59*, 13013.
56. S.-Y. Ding, J. Gao, Q. Wang, Y. Zhang, W.-G. Song, C.-Y. Su, W. Wang, *J. Am. Chem. Soc.* **2011**, *133*, 19816.
57. X. Li, C. Zhang, S. Cai, X. Lei, V. Altoe, F. Hong, J. J. Urban, J. Ciston, E. M. Chan, Y. Liu, *Nat. Commun.* **2018**, *9*, 2998.
58. P. J. Waller, S. J. Lyle, T. M. Osborn Popp, C. S. Diercks, J. A. Reimer, O. M. Yaghi, *J. Am. Chem. Soc.* **2016**, *138*, 15519.
59. S. Karak, S. Kandambeth, B. P. Biswal, H. S. Sasmal, S. Kumar, P. Pachfule, R. Banerjee, *J. Am. Chem. Soc.* **2017**, *139*, 1856.
60. S. Karak, S. Kumar, P. Pachfule, R. Banerjee, *J. Am. Chem. Soc.* **2018**, *140*, 5138.
61. T. Ma, E. A. Kapustin, S. X. Yin, L. Liang, Z. Zhou, J. Niu, L.-H. Li, Y. Wang, J. Su, J. Li, X. Wang, W. D. Wang, W. Wang, J. Sun, O. M. Yaghi, *Science* **2018**, *361*, 48.
62. D. Zhu, L. B. Alemany, W. Guo, R. Verdusco, *Polymer Chem.* **2020**, *11*, 4464.
63. F. J. Uribe-Romo, J. R. Hunt, H. Furukawa, C. Klöck, M. O'Keeffe, O. M. Yaghi, *J. Am. Chem. Soc.* **2009**, *131*, 4570.
64. J. L. Segura, M. J. Mancheño, F. Zamora, *Chem. Soc. Rev.* **2016**, *45*, 5635.
65. R.-R. Liang, S.-Y. Jiang, A. Ru-Han, X. Zhao, *Chem. Soc. Rev.* **2020**, *49*, 3920.
66. E. Vitaku, W. R. Dichtel, *J. Am. Chem. Soc.* **2017**, *139*, 12911.
67. M. Matsumoto, R. R. Dasari, W. Ji, C. H. Feriante, T. C. Parker, S. R. Marder, W. R. Dichtel, *J. Am. Chem. Soc.* **2017**, *139*, 4999.
68. B. J. Smith, A. C. Overholts, N. Hwang, W. R. Dichtel, *Chem. Commun.* **2016**, *52*, 3690.
69. F. Haase, B. V. Lotsch, *Chem. Soc. Rev.* **2020**, *49*, 8469.
70. A. López-Magano, B. Ortín-Rubio, I. Imaz, D. MasPOCH, J. Alemán, R. Mas-Ballesté, *ACS Catal.* **2021**, *11*, 12344.
71. S. Kandambeth, A. Mallick, B. Lukose, M. V. Mane, T. Heine, R. Banerjee, *J. Am. Chem. Soc.* **2012**, *134*, 19524.
72. F. Haase, E. Troschke, G. Savasci, T. Banerjee, V. Duppel, S. Dörfler, M. M. J. Grundei, A. M. Burow, C. Ochsenfeld, S. Kaskel, B. V. Lotsch, *Nat. Commun.* **2018**, *9*, 2600.
73. P. G. Cozzi, *Chem. Soc. Rev.* **2004**, *33*, 410.
74. D. Stewart, D. Antypov, M. S. Dyer, M. J. Pitcher, A. P. Katsoulidis, P. A. Chater, F. Blanc, M. J. Rosseinsky, *Nat. Commun.* **2017**, *8*, 1102.
75. H.-L. Qian, F.-L. Meng, C.-X. Yang, X.-P. Yan, *Angew. Chem. Int. Ed.* **2020**, *59*, 17607.
76. R. Upadhyay, R. Rana, S. K. Maurya, *ChemCatChem* **2021**, *13*, 1867.
77. L. Grunenberg, G. Savasci, M. W. Terban, V. Duppel, I. Moudrakovski, M. Etter, R. E. Dinnebier, C. Ochsenfeld, B. V. Lotsch, *J. Am. Chem. Soc.* **2021**, *143*, 3430.
78. S.-Y. Jiang, S.-X. Gan, X. Zhang, H. Li, Q.-Y. Qi, F.-Z. Cui, J. Lu, X. Zhao, *J. Am. Chem. Soc.* **2019**, *141*, 14981.
79. M. Zhang, Y. Li, W. Yuan, X. Guo, C. Bai, Y. Zou, H. Long, Y. Qi, S. Li, G. Tao, C. Xia, L. Ma, *Angew. Chem. Int. Ed.* **2021**, *60*, 12396.
80. H. Liu, J. Chu, Z. Yin, X. Cai, L. Zhuang, H. Deng, *Chem* **2018**, *4*, 1696.
81. H. M. El-Kaderi, J. R. Hunt, J. L. Mendoza-Cortés, A. P. Côté, E. R. Taylor, M. O'Keeffe, O. M. Yaghi, *Science* **2007**, *316*, 268.
82. J. R. Hunt, C. J. Doonan, J. D. LeVangie, A. P. Côté, O. M. Yaghi, *J. Am. Chem. Soc.* **2008**, *130*, 11872.
83. A. P. Côté, A. I. Benin, N. W. Ockwig, M. O'Keeffe, A. J. Matzger, O. M. Yaghi, *Science* **2005**, *310*, 1166.
84. K. T. Jackson, T. E. Reich, H. M. El-Kaderi, *Chem. Commun.* **2012**, *48*, 8823.
85. Y. Du, H. Yang, J. M. Whiteley, S. Wan, Y. Jin, S.-H. Lee, W. Zhang, *Angew. Chem. Int. Ed.* **2016**, *55*, 1737.
86. L. M. Lanni, R. W. Tilford, M. Bharathy, J. J. Lavigne, *J. Am. Chem. Soc.* **2011**, *133*, 13975.
87. M. Calik, T. Sick, M. Dogru, M. Döblinger, S. Datz, H. Budde, A. Hartschuh, F. Auras, T. Bein, *J. Am. Chem. Soc.* **2016**, *138*, 1234.
88. E. L. Spitler, W. R. Dichtel, *Nat. Chem.* **2010**, *2*, 672.
89. N. L. Campbell, R. Clowes, L. K. Ritchie, A. I. Cooper, *Chem. Mater.* **2009**, *21*, 204.
90. X. Zhuang, W. Zhao, F. Zhang, Y. Cao, F. Liu, S. Bi, X. Feng, *Polym. Chem.* **2016**, *7*, 4176.
91. E. Jin, M. Asada, Q. Xu, S. Dalapati, M. A. Addicoat, M. A. Brady, H. Xu, T. Nakamura, T. Heine, Q. Chen, D. Jiang, *Science* **2017**, *357*, 673.
92. H. Lyu, C. S. Diercks, C. Zhu, O. M. Yaghi, *J. Am. Chem. Soc.* **2019**, *141*, 6848.
93. S. Wei, F. Zhang, W. Zhang, P. Qiang, K. Yu, X. Fu, D. Wu, S. Bi, F. Zhang, *J. Am. Chem. Soc.* **2019**, *141*, 14272.
94. S. Bi, C. Yang, W. Zhang, J. Xu, L. Liu, D. Wu, X. Wang, Y. Han, Q. Liang, F. Zhang, *Nat. Commun.* **2019**, *10*, 2467.
95. D. L. Pastoetter, S. Xu, M. Borrelli, M. Addicoat, B. P. Biswal, S. Paasch, A. Dianat, H. Thomas, R. Berger, S. Reineke, E. Brunner, G. Cuniberti, M. Richter, X. Feng, *Angew. Chem. Int. Ed.* **2020**, *59*, 23620.
96. E. Jin, K. Geng, K. H. Lee, W. Jiang, J. Li, Q. Jiang, S. Irle, D. Jiang, *Angew. Chem. Int. Ed.* **2020**, *59*, 12162.
97. J. Xu, Y. He, S. Bi, M. Wang, P. Yang, D. Wu, J. Wang, F. Zhang, *Angew. Chem. Int. Ed.* **2019**, *58*, 12065.
98. A. Acharjya, P. Pachfule, J. Roeser, F.-J. Schmitt, A. Thomas, *Angew. Chem. Int. Ed.* **2019**, *58*, 14865.
99. S. Bi, P. Thiruvengadam, S. Wei, W. Zhang, F. Zhang, L. Gao, J. Xu, D. Wu, J.-S. Chen, F. Zhang, *J. Am. Chem. Soc.* **2020**, *142*, 11893.
100. T. Sun, J. Xie, W. Guo, D.-S. Li, Q. Zhang, *Adv. Energy Mater.* **2020**, *10*, 1904199.
101. X.-X. Luo, W.-H. Li, H.-J. Liang, H.-X. Zhang, K.-D. Du, X.-T. Wang, X.-F. Liu, J.-P. Zhang, X.-L. Wu, *Angew. Chem. Int. Ed.* **2022**, *61*, e202117661.
102. Z. Lei, Q. Yang, Y. Xu, S. Guo, W. Sun, H. Liu, L.-P. Lv, Y. Zhang, Y. Wang, *Nat. Commun.* **2018**, *9*, 576.
103. Z. Wang, S. Gu, L. Cao, L. Kong, Z. Wang, N. Qin, M. Li, W. Luo, J. Chen, S. Wu, G. Liu, H. Yuan, Y. Bai, K. Zhang, Z. Lu, *ACS Appl. Mater. Interfaces* **2021**, *13*, 514.
104. G. Zhao, L. Xu, J. Jiang, Z. Mei, Q. An, P. Lv, X. Yang, H. Guo, X. Sun, *Nano Energy* **2022**, *92*, 106756.
105. L. Gong, X. Yang, Y. Gao, G. Yang, Z. Yu, X. Fu, Y. Wang, D. Qi, Y. Bian, K. Wang, J. Jiang, *J. Mater. Chem. A* **2022**, *10*, 16595.
106. J. W. Colson, W. R. Dichtel, *Nat. Chem.* **2013**, *5*, 453.
107. S. M. J. Rogge, A. Bavykina, J. Hajek, H. Garcia, A. I. Olivos-Suarez, A. Sepúlveda-Escribano, A. Vimont, G. Clet, P. Bazin, F. Kapteijn, M. Daturi, E. V. Ramos-Fernandez, I. X. F. X. Llabrés, V. Van Speybroeck, J. Gascon, *Chem. Soc. Rev.* **2017**, *46*, 3134.
108. P. Puthiaraj, Y. R. Lee, S. Q. Zhang, W. S. Ahn, *J. Mater. Chem. A* **2016**, *4*, 16288.
109. N. Huang, P. Wang, D. L. Jiang, *Nat. Rev. Mater.* **2016**, *1*, 16068.
110. W. Tu, Y. Xu, S. Yin, R. Xu, *Adv. Mater.* **2018**, *30*, 1707582.
111. A. Aijaz, Q.-L. Zhu, N. Tsumori, T. Akita, Q. Xu, *Chem. Commun.* **2015**, *51*, 2577.
112. V. Stavila, R. Parthasarathi, R. W. Davis, F. El Gabaly, K. L. Sale, B. A. Simmons, S. Singh, M. D. Allendorf, *ACS Catal.* **2016**, *6*, 55.
113. J.-W. Zhang, G.-P. Lu, C. Cai, *Green Chem.* **2017**, *19*, 4538.
114. V. R. Bakuru, D. Davis, S. B. Kalidindi, *Dalton Trans.* **2019**, *48*, 8573.
115. G. Guo, D. Chen, T. Ahmed, X. Dou, K. Chen, W. Li, *Fuel* **2021**, *306*, 121599.
116. W. Jiang, J.-P. Cao, J.-X. Xie, L. Zhao, C. Zhang, C. Zhu, X.-Y. Zhao, Y.-P. Zhao, J.-L. Zhang, *Catal. Sci. Technol.* **2022**, *12*, 488.
117. J.-Y. Lin, H.-K. Lai, K.-Y. A. Lin, *Chem. Pap.* **2018**, *72*, 2315.
118. H.-R. Tian, Y.-W. Liu, Z. Zhang, S.-M. Liu, T.-Y. Dang, X.-H. Li, X.-W. Sun, Y. Lu, S.-X. Liu, *Green Chem.* **2020**, *22*, 248.
119. H.-K. Lai, Y.-Z. Chou, M.-H. Lee, K.-Y. A. Lin, *Chem. Eng. J.* **2018**, *332*, 717.
120. Q. Xu, Q. Wang, L.-P. Xiao, X.-Y. Li, X. Xiao, M.-X. Li, M.-R. Lin, Y.-M. Zhao, R.-C. Sun, *J. Mater. Chem. A* **2023**, *11*, 23809.
121. Q. Wang, L.-P. Xiao, Y.-H. Lv, W.-Z. Yin, C.-J. Hou, R.-C. Sun, *ACS Catal.* **2022**, *12*, 11899.
122. Q. Wang, T. Su, Y. Wang, Y. Chen, X. Lu, R. Ma, Y. Fu, W. Zhu, *ACS Sustain. Chem. Eng.* **2020**, *8*, 17008.

123. J. Zhu, F. Chen, Z. Zhang, M. Li, Q. Yang, Y. Yang, Z. Bao, Q. Ren, *ACS Sustain. Chem. Eng.* **2019**, 7, 12955.
124. M. Fujita, L. Que Jr, *Adv. Synth. Catal.* **2004**, 346, 190.
125. J. Pan, J. Fu, X. Lu, *Energy Fuels* **2015**, 29, 4503.
126. R. V. Lloyd, P. M. Hanna, R. P. Mason, *Free Radic. Biol. Med.* **1997**, 22, 885.
127. M. Shilpy, M. A. Ehsan, T. H. Ali, S. B. Abd Hamid, M. E. Ali, *RSC Adv.* **2015**, 5, 79644.
128. X. Pang, C. Wan, M. Wang, Z. Lin, *Angew. Chem. Int. Ed.* **2014**, 53, 5524.
129. S. Saha, S. B. Abd Hamid, *RSC Adv.* **2016**, 6, 96314.
130. N. J. Hill, J. M. Hoover, S. S. Stahl, *J. Chem. Educ.* **2013**, 90, 102.
131. J. M. Hoover, S. S. Stahl, *J. Am. Chem. Soc.* **2011**, 133, 16901.
132. J.-Y. Lin, H. Wang, W. D. Oh, J. Lee, E. Kwon, S. You, C.-H. Lin, K.-Y. A. Lin, *Chem. Eng. J.* **2021**, 411, 128605.
133. S. Ju, M. Yusuf, S. Jang, H. Kang, S. Kim, K. H. Park, *Chem. Eur. J.* **2019**, 25, 7852.
134. B.-C. Li, J.-Y. Lin, J. Lee, E. Kwon, B. X. Thanh, X. Duan, H. H. Chen, H. Yang, K.-Y. A. Lin, *Colloids Surf. A: Physicochem. Eng. Asp.* **2021**, 631, 127639.
135. T. S. Hansen, I. Sádaba, E. J. García-Suárez, A. Riisager, *Appl. Catal. A: Gen.* **2013**, 456, 44.
136. A. K. Kar, S. P. Kaur, T. J. D. Kumar, R. Srivastava, *Catal. Sci. Technol.* **2020**, 10, 6892.
137. E. V. Ramos-Fernandez, C. Pieters, B. van der Linden, J. Juan-Alcañiz, P. Serra-Crespo, M. W. G. M. Verhoeven, H. Niemantsverdriet, J. Gascon, F. Kapteijn, *J. Catal.* **2012**, 289, 42.
138. H.-L. Jiang, T. Akita, T. Ishida, M. Haruta, Q. Xu, *J. Am. Chem. Soc.* **2011**, 133, 1304.
139. M. Ahsan Usman, M. Naeem, M. Saeed, M. Zaheer, *Inorg. Chim. Acta* **2021**, 521, 120305.
140. G. Férey, C. Mellot-Draznieks, C. Serre, F. Millange, J. Dutour, S. Surblé, I. Margiolaki, *Science* **2005**, 309, 2040.
141. R. Liang, F. Jing, L. Shen, N. Qin, L. Wu, *Nano Res.* **2015**, 8, 3237.
142. H. Zhang, Z. Yi, S. Fu, C. Li, L. A. Lucia, Q. Liu, *Appl. Catal. B: Environ.* **2023**, 322, 122128.
143. Y. Song, Z. Li, P. Ji, M. Kaufmann, X. Feng, J. S. Chen, C. Wang, W. Lin, *ACS Catal.* **2019**, 9, 1578.
144. J.-A. Jiang, C. Chen, Y. Guo, D.-H. Liao, X.-D. Pan, Y.-F. Ji, *Green Chem.* **2014**, 16, 2807.
145. M. Saidi, F. Samimi, D. Karimipourfard, T. Nimmanwudipong, B. C. Gates, M. R. Rahimpour, *Energy Environ. Sci.* **2014**, 7, 103.
146. Q. Sun, M. Chen, B. Aguila, N. Nguyen, S. Ma, *Faraday Discuss.* **2017**, 201, 317.
147. Q. Wang, N. Gupta, G. Wen, S. B. A. Hamid, D. S. Su, *J. Energy Chem.* **2017**, 26, 8.
148. H. Liu, T. Jiang, B. Han, S. Liang, Y. Zhou, *Science* **2009**, 326, 1250.
149. M. R. DeStefano, T. Islamoglu, S. J. Garibay, J. T. Hupp, O. K. Farha, *Chem. Mater.* **2017**, 29, 1357.
150. R. C. Klet, Y. Liu, T. C. Wang, J. T. Hupp, O. K. Farha, *J. Mater. Chem. A* **2016**, 4, 1479.
151. W. Wang, T. Sheng, S. Chen, Z. Xiang, F. Zhou, W. Zhu, H. Wang, *Chem. Eng. J.* **2023**, 453, 139711.
152. X. Tong, P. Guo, S. Liao, S. Xue, H. Zhang, *Green Chem.* **2019**, 21, 5828.
153. X.-G. Si, Y.-P. Zhao, Q.-L. Song, J.-P. Cao, R.-Y. Wang, X.-Y. Wei, *React. Chem. Eng.* **2020**, 5, 886.
154. T. Prasomsri, M. Shetty, K. Murugappan, Y. Román-Leshkov, *Energy Environ. Sci.* **2014**, 7, 2660.
155. M. Grilc, G. Veryasov, B. Likozar, A. Jesih, J. Levec, *Appl. Catal. B: Environ.* **2015**, 163, 467.
156. X. Ma, R. Ma, W. Hao, M. Chen, F. Yan, K. Cui, Y. Tian, Y. Li, *ACS Catal.* **2015**, 5, 4803.
157. F. Ge, H. Xia, J. Li, Y. Xue, J. Su, X. Yang, J. Jiang, M. Zhou, *Chem. Eng. J.* **2023**, 473, 145375.
158. Q. Guo, J. Mao, S. Li, J. Yin, Y. Lv, J. Zhou, *Nanomaterials* **2022**, 12, 3388.
159. H. Xia, C. Chen, P. Liu, M. Zhou, J. Jiang, *Sustain. Energy Fuels* **2020**, 4, 5709.
160. P. Liu, C. Chen, M. Zhou, J. Xu, H. Xia, S. Shang, J. Jiang, *Sustain. Energy Fuels* **2021**, 5, 1809.
161. C. Chen, P. Liu, M. Zhou, J. Li, H. Xia, J. Jiang, *J. Energy Inst.* **2021**, 99, 105.
162. C. Li, X. Zhao, A. Wang, G. W. Huber, T. Zhang, *Chem. Rev.* **2015**, 115, 11559.
163. Y. Ma, Z. Du, J. Liu, F. Xia, J. Xu, *Green Chem.* **2015**, 17, 4968.
164. S. Son, F. D. Toste, *Angew. Chem. Int. Ed.* **2010**, 49, 3791.
165. S. K. Hanson, R. Wu, L. A. P. Silks, *Angew. Chem. Int. Ed.* **2012**, 51, 3410.
166. B. Sedai, C. Díaz-Urrutia, R. T. Baker, R. Wu, L. A. P. Silks, S. K. Hanson, *ACS Catal.* **2011**, 1, 794.
167. M. Wang, L. H. Li, J. M. Lu, H. J. Li, X. C. Zhang, H. F. Liu, N. C. Luo, F. Wang, *Green Chem.* **2017**, 19, 702.
168. B. Bianic, J. J. Bozell, *Org. Lett.* **2013**, 15, 2730.
169. C. Crestini, P. Pro, V. Neri, R. Saladino, *Bioorg. Med. Chem.* **2005**, 13, 2569.
170. W. Deng, H. Zhang, X. Wu, R. Li, Q. Zhang, Y. Wang, *Green Chem.* **2015**, 17, 5009.
171. J. F. Blandez, S. Navalón, M. Alvaro, H. Garcia, *ChemCatChem* **2015**, 7, 3020.
172. Y. Yang, H. Fan, J. Song, Q. Meng, H. Zhou, L. Wu, G. Yang, B. Han, *Chem. Commun.* **2015**, 51, 4028.
173. Y. Yang, H. Fan, Q. Meng, Z. Zhang, G. Yang, B. Han, *Chem. Commun.* **2017**, 53, 8850.
174. J. Long, Y. Xu, T. Wang, Z. Yuan, R. Shu, Q. Zhang, L. Ma, *Appl. Energy* **2015**, 141, 70.
175. J. Long, Q. Zhang, T. Wang, X. Zhang, Y. Xu, L. Ma, *Bioresour. Technol.* **2014**, 154, 10.
176. A. Toledano, L. Serrano, J. Labidi, *Fuel* **2014**, 116, 617.
177. M. Wang, J. Lu, X. Zhang, L. Li, H. Li, N. Luo, F. Wang, *ACS Catal.* **2016**, 6, 6086.
178. H. Zhou, H. Xu, Y. Liu, *Appl. Catal. B: Environ.* **2019**, 244, 965.
179. R. Vidruk, M. V. Landau, M. Herskowitz, M. Talianker, N. Frage, V. Ezersky, N. Froumin, *J. Catal.* **2009**, 263, 196.
180. J. Huang, Y. Wang, J. Zheng, W.-L. Dai, K. Fan, *Appl. Catal. B: Environ.* **2011**, 103, 343.
181. H. Zhou, B. Han, T. Liu, X. Zhong, G. Zhuang, J. Wang, *Green Chem.* **2017**, 19, 3585.
182. A. Nougima, T. Mitsudome, T. Mizugaki, K. Jitsukawa, K. Kaneda, *Green Chem.* **2013**, 15, 608.
183. J. J. Moreno, M. F. Espada, J. Campos, J. López-Serrano, S. A. Macgregor, E. Carmona, *J. Am. Chem. Soc.* **2019**, 141, 2205.
184. B. G. Hashiguchi, K. J. H. Young, M. Yousufuddin, W. A. Goddard III, R. A. Periana, *J. Am. Chem. Soc.* **2010**, 132, 12542.
185. R. Chaudhary, P. L. Dhepe, *Green Chem.* **2017**, 19, 778.
186. S. Dabral, J. Mottweiler, T. Rinesch, C. Bolm, *Green Chem.* **2015**, 17, 4908.
187. X. Erdocia, R. Prado, M. Á. Corcuera, J. Labidi, *Biomass Bioenergy* **2014**, 66, 379.
188. A. Toledano, L. Serrano, J. Labidi, *J. Chem. Technol. Biotechnol.* **2012**, 87, 1593.
189. H. Konnerth, J. Zhang, D. Ma, M. H. G. Precht, N. Yan, *Chem. Eng. Sci.* **2015**, 123, 155.
190. T. Renders, W. Schutyser, S. Van den Bosch, S.-F. Koelewijn, T. Vangeel, C. M. Courtin, B. F. Sels, *ACS Catal.* **2016**, 6, 2055.
191. H. Li, G. Song, *ACS Catal.* **2019**, 9, 4054.
192. G. Zhu, S. Shi, M. Liu, L. Zhao, M. Wang, X. Zheng, J. Gao, J. Xu, *ACS Appl. Mater. Interfaces* **2018**, 10, 12612.
193. L. Zhao, S. Shi, G. Zhu, M. Liu, J. Gao, J. Xu, *Green Chem.* **2019**, 21, 6707.
194. G. Zhu, S. Shi, L. Zhao, M. Liu, J. Gao, J. Xu, *ACS Catal.* **2020**, 10, 7526.

How to cite this article: Q. Huang, P. Wu, X.-F. Li, Y.-R. Wang, D. Tian, Y.-Q. Lan, *Aggregate* **2024**, e525. <https://doi.org/10.1002/agt2.525>

AUTHOR BIOGRAPHIES



Qing Huang received her BS degree from Jiangxi Normal University in 2015. She subsequently obtained her PhD degree (2020) under the supervision of Prof. Ya-Qian Lan in Nanjing Normal University. She worked with Prof. Ya-Qian Lan and Prof. Yue-Peng Cai in South China

Normal University as a postdoctoral fellow during 2020–2023. She is now an associate professor in Nanjing Forestry University. Her research interest focuses on the synthesis and catalysis applications of porous crystalline materials including metal-organic frameworks and covalent organic frameworks.



Dan Tian received her PhD in college of Chemistry from Nankai University (China) under the supervision of Prof. Xianhe Bu in 2015. She then studied for 2 years at the Nanjing Tech University in the area of lanthanide-doped upconversion metal-organic frameworks and pho-

tophysical properties of solid-state boron-dipyrromethene dyes. Then, she moved to Nanyang Technological University (Singapore) as a postdoctoral fellowship in School of Materials Science and Engineering from 2017 to 2019. She is currently a professor at Nanjing Forestry University. Her research interest now focuses on development and utilization of biomass materials.



Ya-Qian Lan was born in 1978 in Jilin, China. He received his BS and PhD (2009) from Faculty of Chemistry, Northeast Normal University, under the supervision of Prof. Zhong-Min Su. In 2010, he worked as a Japan Society for the Promotion of Science (JSPS) post-

doctoral fellow at National Institute of Advanced Industrial Science and Technology (AIST). Since the fall of 2012, he has been a Professor of Chemistry at Nanjing Normal University. His current research interests focus on synthesis of porous crystalline materials and catalytic research related to energy applications.